Journal
of
The Franklin Institute

DEVOTED TO

SCIENCE AND THE MECHANIC ARTS

MANAGING EDITOR, NANCY S. GLENN

ASSOCIATE EDITORS:

CHARLES B. BAZZONI
WILLIAM H. BOGHOSIAN
CHARLES L. CRITCHFIELD
RUPEN EKSERGIAN
VIRGIL MORING FAIRES
PAUL D. FOOTE
DUNSTAN GRAHAM
WALTER C. JOHNSON
Y. H. KU
ROBERT S. LIVINGSTON
F. J. MURRAY
C. J. STAUD
W. F. G. SWANN
HUGH S. TAYLOR
MERLE A. TUVE

COMMITTEE ON PUBLICATIONS:

HENRY B. ALLEN
LIONEL F. LEVY, CHAIRMAN
CLARENCE L. JORDAN
PHILIP H. WARD, JR.

VOL. 271—Nos. 1621–1626
(136th Year)

JANUARY–JUNE, 1961

PHILADELPHIA
THE FRANKLIN INSTITUTE
Benjamin Franklin Parkway at 20th Street
1961

LANCASTER PRESS, INC., LANCASTER, PA.

Journal
of
The Franklin Institute
Devoted to Science and the Mechanic Arts

Vol. 271 JANUARY, 1961 No. 1

SPIRAL STELLAR NEBULAE AND COSMIC GAS JETS*

BY

C. E. R. BRUCE[1]

SUMMARY

The paper describes the successful culmination of a search for photographic evidence of the existence of spiral *stellar* nebulae, initiated by the writer's electrical discharge theory of astrophysical atmospheric phenomena, as applied to some types of bright line stars. This theory for the first time offers a satisfactory explanation for the general form and the gas movements observed in planetary nebulae. It elucidates the general nature of cosmic gas jets, concerning which quite erroneous assumptions are made in relation to those in the sun's atmosphere which cause *magnetic storms*. Applied to galactic nebulae, the theory explains the strange discontinuity recently observed in the gas movements in the barred spiral nebula NGC 1097.

1. SPIRAL STELLAR NEBULAE

The forces which are operative in the formation of the extra-galactic spiral nebulae have remained a mystery since the first discovery (1)[2] of their spiral structure, be it noted, by Lord Rosse, President of the Royal Society in 1845, using his 6-ft. diameter "leviathan of Parsonstown." To these the writer has recently added for like consideration spiral nebulae on a stellar scale (2a), the existence of which had remained apparently unnoticed and without comment since they were photographed at Lick Observatory by H. D. Curtis (3) in 1918.

The existence of these stellar spiral nebulae was recently "discovered" as the result of a search of the literature for just such photographic evidence of their existence.

The first step which originated this search was the suggestion that the well-known group of P Cygni stars, which have been the special

* Based on several recent Electric Research Association Reports, including Ref. Z/T 117, Z/T 125 and Z/T 132.

[1] Electrical Research Association Laboratories, Leatherhead, Surrey, England.

[2] The boldface numbers in parentheses refer to the references appended to this paper.

(Note—The Franklin Institute is not responsible for the statements and opinions advanced by contributors in the JOURNAL.)

study, for example, of C. S. Beals, Dominion Astronomer of Canada, are stars essentially similar to R Monocerotis, better known as Hubble's Variable Nebula, shown in Fig. 1. This photograph has the additional interest that it was the first official photograph taken by Hubble himself using the 200-in. Hale telescope at Mount Palomar Observatory on January 26, 1949. However, in the P Cygni stars the associated cometary nebula, it is suggested, is directed toward us.

On the electrical discharge or "thunderstorm" theory of these astrophysical atmospheric phenomena (2b, c) these are stars in which the atmospheric gas has been largely collected along the discharge channel of an old nova-like outburst by magnetic pinch effect, just as

FIG. 1. Hubble's variable nebula (R Monocerotis).

the pressure is increased in the laboratory arc discharge by the same effect. It is therefore of note that P Cygni is indeed an old nova. It is this magnetic pinch effect which, for example, mainly renders possible electric arc welding. The pressure gradient so generated from the current constriction at the cathode spot along the axis of the arc, causes a jet of hot gas to flow and entrain the metal of the welding electrode and carry it over to the anode, as will be seen in Fig. 2, a photograph taken from a high speed film of the welding process taken by Needham in these laboratories.

This axial pressure rise in an electrical discharge is proportional to the product of the current and the current density. Both these quantities decrease as the discharge is propagated outwards in these stellar

atmospheric electrical discharges, so that outward jets of hot gas emit the bright lines in the stars' spectra which are therefore displaced towards the violet in these stars in which the nebulae are directed towards us, as it is suggested it is in P Cygni.

There exist, however, many stars in which the bright emission lines are double, with components displaced towards both the red and the violet. These, it seemed to the writer, could be stars in which there had been two major discharges in the original outburst, just as is always observed in the galactic spiral nebulae (2d). Since photographs of stars like Hubble's Variable Nebula exist, and will account for these stars having a spectrum of single bright emission components, it seemed

FIG. 2. High speed photograph of the arc welding process.

quite likely that some stars might sometime have been photographed with two such old discharge channels, if the proposed explanation of this type of stellar spectrum is correct. Enquiry from a few astronomical friends brought from Dr. Merrill at Mount Wilson Observatory a reference to the paper by Curtis already referred to (3), which contains a profusion of examples of just such pairs of old discharge channels as the theory had suggested might exist. Some of these are shown in Fig. 3, and it was quite exciting to find that in some of these the two discharge channels had assumed a spiral form, for example NGC 4361, while in others like NGC 2452 and NGC 6778, they showed a barred-spiral form,

exactly analogous to what is observed when the corresponding outbursts occur on a galactic scale. The view of spiral galactic nebulae has been elaborated in a recent E.R.A. Report (2d). In contrast to the galactic discharges, the two discharge channels remain straight in the majority

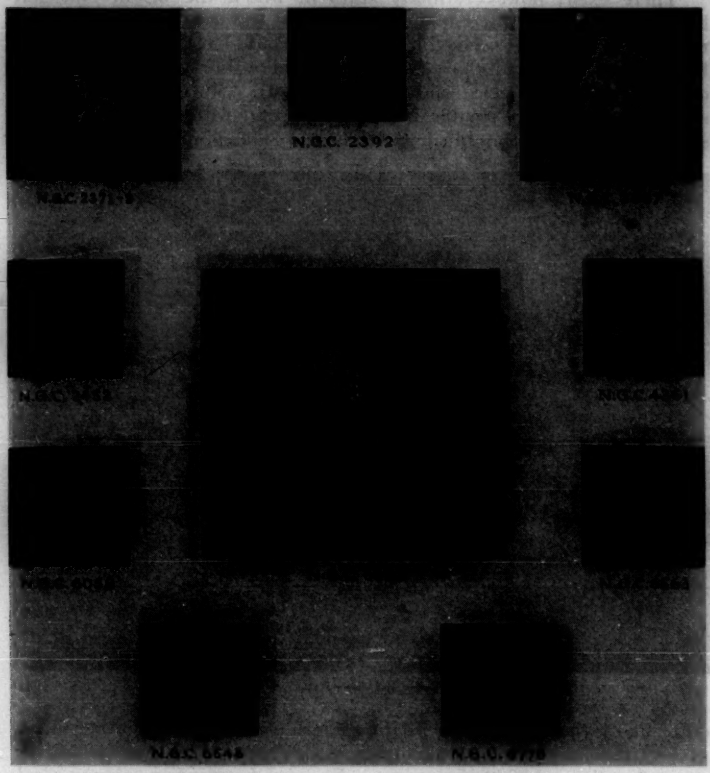

FIG. 3. Photographs of planetary nebulae (Curtis (3)).

of stellar outbursts. In others they remain straight over a proportion of their length before turning off into a spiral form, when the result is a barred-spiral nebula.

This duality of discharge channel is such a marked characteristic of these planetary nebulae that Curtis himself had offered an explanation in terms of matter falling in towards the star from the two poles. It

will be seen that, in contrast to the explanation now offered, this would lead to the *red* component of the lines being the brighter in those stars possessing a spectrum of pairs of bright components, since it would be emitted by the arm on the star's nearer side. Dr. Merrill in two papers (**4a, b**) has referred to twenty stars possessing spectra with

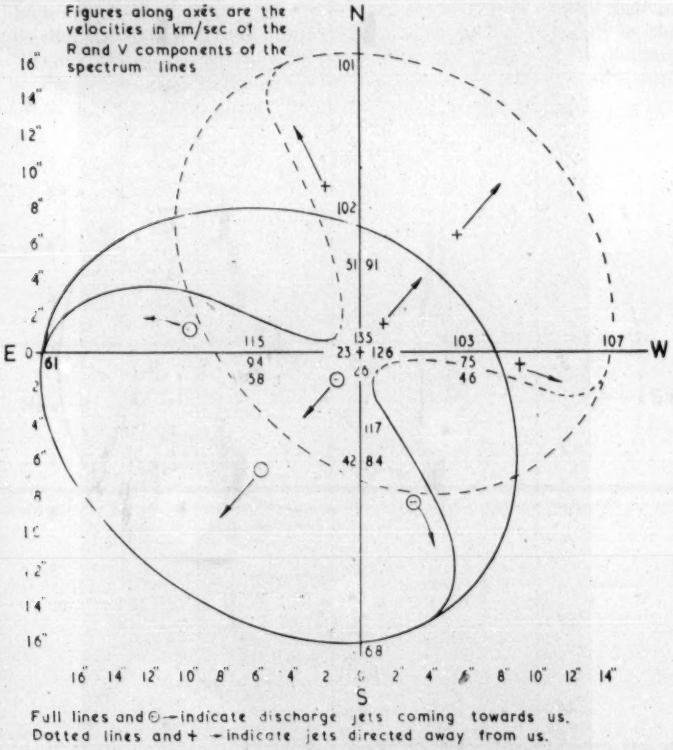

FIG. 4. Diagrammatic representation of the gas jets in NGC 2392.

pairs of bright emission components in which he could compare the relative brightnesses of the two components. In thirteen of these the ***violet*** component was the brighter, in six the two components were approximately equal, and in only one was the red component of the lines the brighter, in accord with the prediction of the new theory, and

quite the reverse of what is to be expected were Curtis's suggestion correct.

2. GAS MOVEMENTS IN THE PLANETARY NEBULAE

The theory also affords an explanation for the gas movements observed in these nebulae, a study of which was made at Lick Observatory

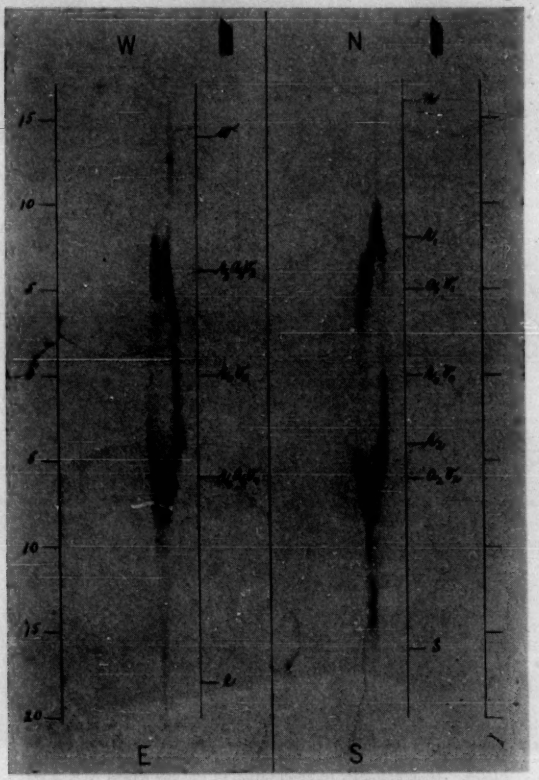

FIG. 5. Moore's drawings of the N_1 line in NGC 2392, with the slit along (*a*) the minor axis and (*b*) the major axis.

by Campbell and Moore (5) and published at the same time as Curtis's photographs. The movements in many of the nebulae defied all efforts at their explanation on the basis of any of the many hypotheses tried by Campbell and Moore, but are, like the photographic and spec-

troscopic observations, also in accord with the new theory. In the diagram in Fig. 4 the figures along the axes are the gas velocities given by Campbell and Moore for NGC 2392, the type nebula of the group which particularly resisted all attempts at their explanation. These will be seen to be at once explicable as deriving from the two gas jets generated by the two diametrically opposed discharge channels. The high velocities of the two jets are seen superposed in the central regions, so that the spectrum lines are there split as in Fig. 5. It is only in the SE and NW quadrants that the two jets are separable. In the diagram in Fig. 6 the figures in the circles are average values derived from Camp-

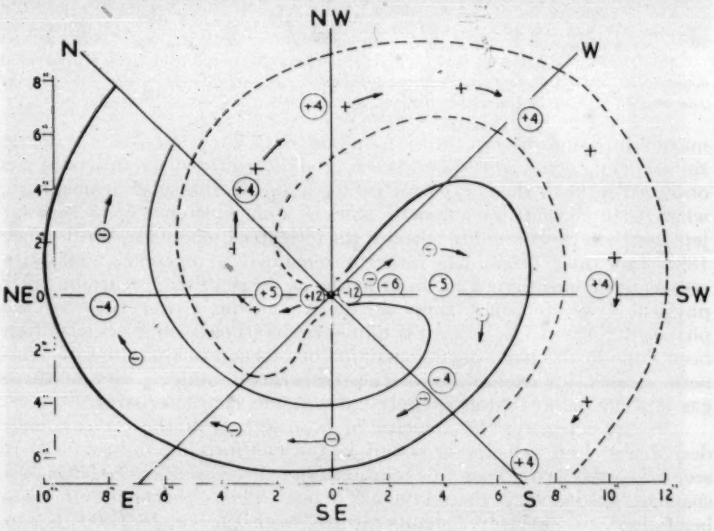

FIG. 6. Diagrammatic representation of the gas jets in NGC 6543.

bell and Moore's measurements for NGC 6543 obtained with the slit of the spectrograph in ten positions across the image of the nebula. These show that in this star the discharges gave rise to spiral jets of gas, as the photograph of the nebula also indicates.

3. COSMIC GAS JETS

So far as the writer is aware, the magnetic pinch effect in electrical discharges is the only physical process which can gather atmospheric

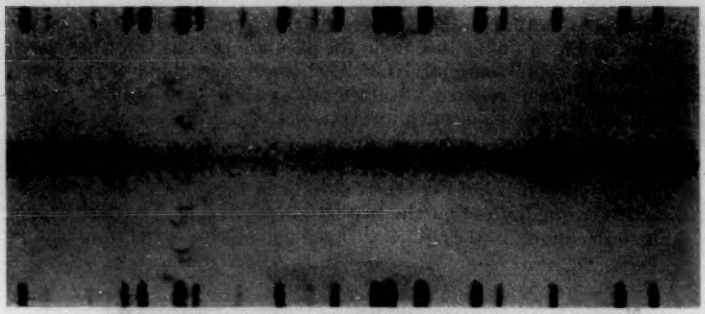

FIG. 7. Photograph of the lines Hα and [N II] λ6583 in the spectrum of the barred spiral nebula NGC 1097. Reproduced with permission of the publisher, from the *Astrophysical Journal*, Vol. 132, p. 30, copyright (1960) by the University of Chicago Press (**8**).

matter into the discrete arms found in both the stellar and galactic spiral nebulae, and at the same time give rise to the discrete jets of gas observed in both these types of nebulae, and in the solar atmosphere, where they account for magnetic storms. The existence of these solar jets has been postulated to account for terrestrial magnetic storms since 1896, but their origin has hitherto remained a mystery, and quite erroneous suppositions have been made, as we shall see, regarding their physical characteristics, suppositions which the writer believes are physically impossible. For it is quite erroneous to assume, as has often been done in the past, particularly in these theoretical studies of magnetic storms, for example, that the temperature and velocity of these gas jets can be treated as entirely independent characteristics.

On the contrary, the velocity of propagation of the jet can only derive from the velocity of sound in the gas forming the jet, and it seemed to the writer that this relationship can be used as the basis of a cosmic "gas-velocity thermometer" (**2e**). This "thermometer" has been used to "measure" temperatures over the range 5000° K. to 4,000,000,000° K., and its "readings" will be seen in Table I (**2f**) to agree well with other methods of estimating the temperature.

TABLE I.—*Gas Temperatures and Velocities in Cosmical Electrical Discharges.*

	Temperature, ° K.		Velocity, km./sec.	
Source	Theory	Observation	Theory	Observation
Long-period variable stars	—	5000° to 10,000°	8.5 to 12	9 (Joy) 11 (Merrill)
Combination spectra star (AX Persei)	8×10^{8}°	$\doteqdot 10^{6}$° (Fe VII, Fe X (?))	—	110 (Merrill)
Extra-galactic nebulae	10^{8}° ~ 10^{9}°	—	1750 to 5400	1800 to 4250 (Seyfert)

Indeed another of the notable recent predictions of the theory was based on this "gas-velocity thermometer," as was recently mentioned in a note in "Reader Opinion" (2g). It derived from the observed velocity of the solar jets which enter the upper atmosphere, and which

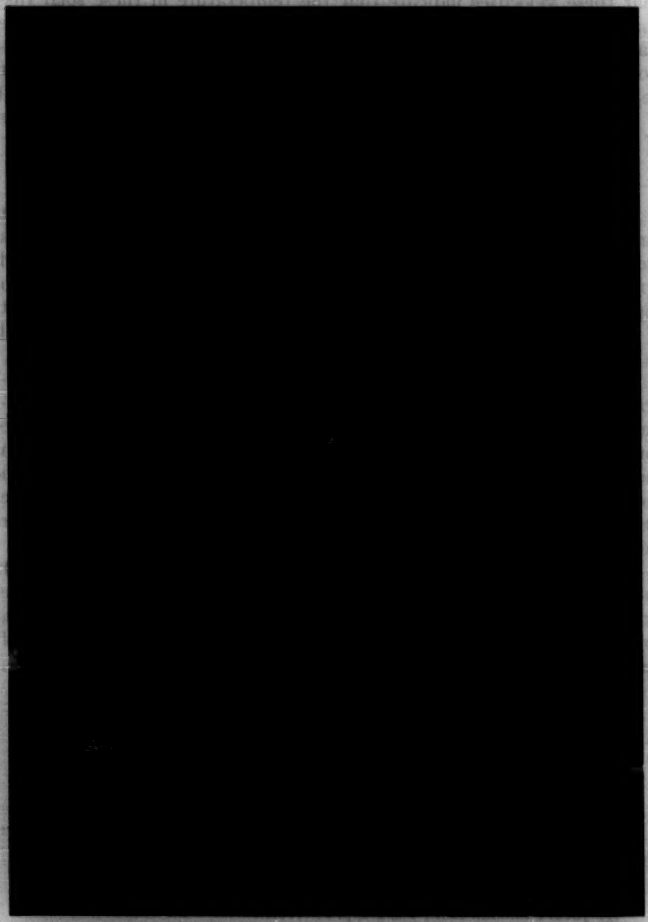

FIG. 8. Photograph of the barred spiral nebula NGC 1097, taken at McDonald Observatory. Reproduced with permission of the publisher, from the *Astrophysical Journal*, Vol. 132, p. 30, copyright (1960) by the University of Chicago Press (8).

cause magnetic storms and aurorae. These velocities, according to Meinel (6), reach 3500 km per second.

It was pointed out in a contribution to the Institution of Electrical Engineers Convention on Thermonuclear Processes in April last year that these velocities indicate that the temperature in these solar discharges must reach over 100,000,000° K. between the sun and the Earth. This prediction had not long to await observational confirmation, for satellite observations made by scientists of the U. S. Navy last year showed that solar flares are accompanied by the emission of 80,000 V X-rays, indicating, as they point out, the existence of temperatures of 100,000,000° K. (7).

4[a]. THE GAS JETS IN BARRED-SPIRAL NEBULA NGC 1097

Support for the theory of spiral and barred-spiral nebulae put forward in the above sections, as applied to galaxies, is contained in a recent paper (8) by Burbidge and Burbidge on the "Motions in Barred Spiral Galaxies." The authors show a photograph, reproduced in Fig. 7, of the emission lines Hα and [N II] λ6583, taken with the slit of the spectrograph more or less along the bar of the barred-spiral galaxy NGC 1097 (Fig. 8).

These emission lines are seen each to comprise two displaced portions separated by the nucleus. The authors' Table 1 of the gas velocities observed along each of these lines shows that these velocities are constant along the bar out to distances ranging from 2".9 to 15".8 on each side of the nucleus, but that the velocities in the line of sight on the two sides of the nucleus differ by about 415 km per sec. As the authors say "there is essentially a velocity discontinuity in the inner part."

This will be seen to be in complete accord with the view of stellar and galactic barred spiral nebulae discussed in the present paper. The two electrical discharges give rise to diametrically opposed jets of gas, flowing outwards along the bar from the center. It is these two jets of gas which give rise to the two displaced portions of the spectrum lines.

REFERENCES

(1) LORD ROSSE, *Phil. Trans. Roy. Soc.*, 1850, p. 505.
(2) C. E. R. BRUCE:
(*a*) *J. I.E.E.*, September, 1960;
(*b*) "A New Approach in Astrophysics and Cosmogony," London, 1944;
(*c*) JOUR. FRANKLIN INST., Vol. 268, p. 425 (1959);
(*d*) "Evolution of Extra-galactic Nebulae and the Origin of Metagalactic Radio Noise," E.R.A. Report Ref. Z/T 117, 1958;
(*e*) *Comptes Rendus*, Vol. 250, p. 61 (1960);
(*f*) *Nature*, Vol. 184, p. 2004 (1959) and the references given therein;
(*g*) JOUR. FRANKLIN INST., Vol. 270, p. 54 (1960).

[a] Section 4 was added to this paper October 19, 1960.

(3) H. D. CURTIS, *Pub. Lick Obs.*, Vol. 13, p. 57 (1918).
(4) P. W. MERRILL:
(*a*) *Astrophysical J.*, Vol. 76, p. 156 (1932) (MWC No. 456);
(*b*) *Astrophysical J.*, Vol. 78, p. 87 (1933) (MWC No. 471).
(5) W. W. CAMPBELL AND J. H. MOORE, *Pub. Lick Obs.*, Vol. 13, p. 75 (1918).
(6) A. B. MEINEL, *Astrophysical J.*, Vol. 113, p. 50 (1951).
(7) JOUR. FRANKLIN INST., Vol. 270, p. 78 (1960).
(8) E. M. BURBIDGE AND G. R. BURBIDGE, *Astrophysical J.*, Vol. 132, p. 30 (1960).

ELLIPTIC FUNCTIONS IN NETWORK SYNTHESIS

BY

S. D. BEDROSIAN[1]

ABSTRACT

Admittedly the Jacobian elliptic functions are not too familiar to the engineer. However, there are occasions when alternate techniques are not as direct or as convenient to solve the approximation problem of network synthesis. The role of elliptic functions in providing a common thread for fundamental concepts involved in Cauer image parameter filters, filters on an insertion loss basis and wide band 90° phase-difference networks is shown. A "unified" design chart for these networks is also included. Additional tabular and graphical data are presented emphasizing extreme parameter values not found in the literature, that is, modular angle $\theta > 89°$, to facilitate getting numerical results. An attempt has been made to provide a practical basis for engineering insight into the synthesis problem. It is also hoped that this paper may serve as an inducement to some of the engineers interested in network synthesis to acquire broader acquaintance with these topics via the references cited.

1. INTRODUCTION

Functional relations between the parameters of Jacobian elliptic functions are well known (1–4).[2] Since the pioneering work of Legendre many of these have been tabulated because of their importance in applied mathematics (4–12). The advent of digital computers has made significant extensions possible (13, 14). In spite of this, their applications to the approximation problem of network synthesis have been handicapped by the coarseness and inadequacy of tabulations hitherto considered to be detailed and complete. The difficulty stems from the doubly periodic nature of the elliptic functions which generally necessitates double entry tables (15–16).

In such network applications the values of the elliptic functions of particular interest and difficulty are those for the modulus k approaching unity. (See Appendix I for a brief summary.) A review of the relationships between parameters, the methods of tabulation and the tabulations themselves reveal that adequate means are at our disposal to surmount many of the handicaps by a judicious choice in presenting the results. Table I and the curves in Figs. 1, 2 and 3 show the relationships germane to network synthesis. In some cases it will be feasible to get the necessary data by graphical interpolation of such curves drawn to much finer scale. Often it will be sufficient to use existing tables augmented by just a few additional calculations with the formulas provided.

Although a fairly lengthy bibliography has been included, it is by no means exhaustive. Rather it is hoped that it will serve as a point

[1] The Institute for Cooperative Research, University of Pennsylvania, Philadelphia, Pa.

[2] The boldface numbers in parentheses refer to the references appended to this paper.

TABLE I.—*Concise Tabulation of Some Elliptic Function Parameters Useful in Network Synthesis.*

90 −θ Degrees	k′	k	K′	K	K′/K	q	θ Degrees
90.00000 00000	1.00000 0000	0.00000 0000	∞	π/2	∞	0.00000 0000	0.00000 00000
60.00000 00000	0.86602 5402	0.50000 0000	2.15651 5648	1.68575 0355	1.27926 1571	0.01797 2387	30.00000 00000
45.00000 00000	0.70710 6782	0.70710 6782	1.85407 4677	1.85407 4677	1.00000 0000	0.04321 3918	45.00000 00000
30.00000 00000	0.50000 0000	0.86602 5402	1.68575 0355	2.15651 5648	0.78170 0961	0.08579 5734	60.00000 00000
15.00000 00000	0.25881 9044	0.96592 5826	1.59814 2002	2.76806 3145	0.57735 0269	0.16303 3535	75.00000 00000
5.73913 15467	0.10000 0000	0.99498 7437	1.57468 8892	3.69563 7363	0.42609 3996	0.26220 8901	84.26086 84533
3.00000 00000	0.05234 5956	0.99862 9530	1.57187 3611	4.33865 3976	0.36229 5223	0.32040 0337	87.00000 00000
1.00000 00000	0.01745 3293	0.99984 7693	1.57091 5958	5.43490 9830	0.28904 1770	0.40330 9306	89.00000 00000
0.57296 73864	0.01000 0000	0.99994 9999	1.57083 5597	5.99158 9341	0.26217 3441	0.43883 0454	89.42703 26136
0.10000 00000	0.00174 5329	0.99999 8477	1.57079 7522	7.73710 6553	0.20302 1311	0.52844 8325	89.90000 00000
0.05729 57910	0.00100 0000	0.99999 9500	1.57079 6720	8.29405 1464	0.18938 8349	0.55153 3022	89.94270 42090
0.01000 00000	0.00017 4533	0.99999 9985	1.57079 6334	10.03968 6581	0.15645 8702	0.61169 0094	89.99000 00000
0.00572 95780	0.00010 0000	0.99999 9995	1.57079 6331	10.59663 4757	0.14823 5394	0.62769 0102	89.99427 04220
0.00100 00000	0.00001 7453	0.99999 9998	1.57079 6327	12.34227 1674	0.12726 9628	0.67043 4462	89.99900 00000
0.00057 29578	0.00001 0000	0.99999 9999	1.57079 6327	12.89921 9826	0.12177 4522	0.68210 8910	89.99942 70422
0.00010 00000	0.00000 1745	1.00000 0000	1.57079 6327	14.64485.6767	0.10725 9248	0.71393 3924	89.99990 00000
0.00005 72958	0.00000 1000	1.00000 0000	1.57079 6327	15.20180 4919	0.10332 9594	0.72280 2333	89.99994 27042
0.00001 00000	0.00000 0175	1.00000 0000	1.57079 6327	16.94744 6791	0.09268 6311	0.74737 9170	89.99999 00000
0.00000 57296	0.00000 0100	1.00000 0000	1.57079 6327	17.50439 0012	0.08973 7279	0.75433 5557	89.99999 42704
0.00000 10000	0.00000 0018	1.00000 0000	1.57079 6327	19.25002 1884	0.08159 9716	0.77387 8865	89.99999 90000
0.00000 05730	0.00000 0010	1.00000 0000	1.57079 6327	19.80697 5105	0.07930 5210	0.77946 7204	89.99999 94270
0.00000 01000	0.00000 0002	1.00000 0000	1.57079 6327	21.55260 6977	0.07288 1964	0.79535 6020	89.99999 99000
0.00000 00573	0.00000 0001	1.00000 0000	1.57079 6327	22.10956 0198	0.07104 6023	0.79995 6712	89.99999 99427
0.00000 00100	0.00000 0000	1.00000 0000	1.57079 6327	23.88519 2070	0.06576 4442	0.81334 0786	89.99999 99900
0.00000 00057	0.00000 0000	1.00000 0000	1.57079 6327	24.41214 5291	0.06434 4870	0.81697 6155	89.99999 99943
0	0	1.00000 0000	π/2	∞	0	1.00000 0000	90.00000 0000

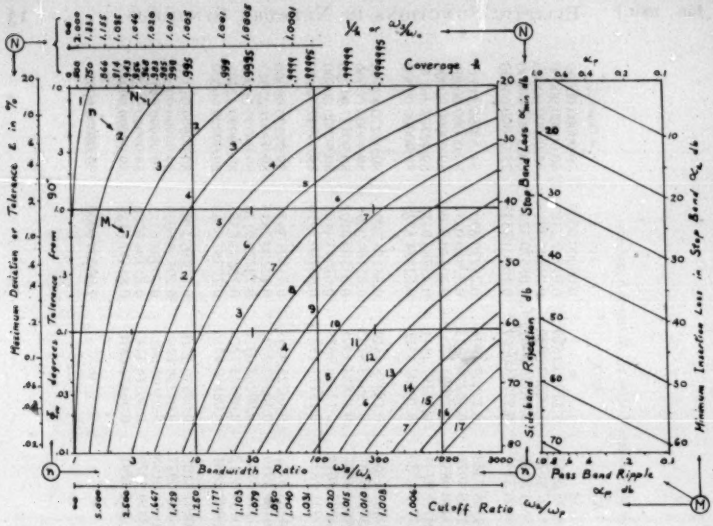

FIG. 1. Unified network design chart.

Use *N* scales for image parameter filters
Use *M* scales for elliptic function symmetrical filters
Use *n* scales for 90° phase-difference networks

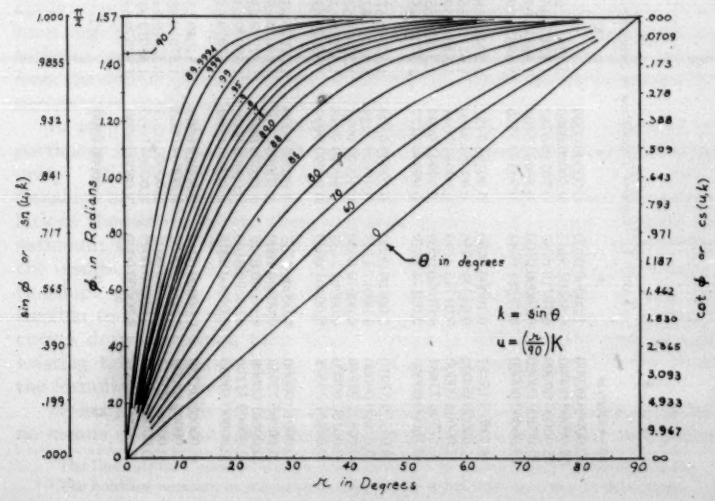

FIG. 2. Elliptic functions yielding normalized critical frequencies for network synthesis.

of departure for the several topics touched upon in this concise treatment of a broad subject.

2. APPROXIMATION PROCEDURE

The approximation problem of network synthesis is concerned with the derivation of a transfer function based on performance specifications. An approximation is usually required since the specifications tend to be idealized and often are not quite realizable as a finite physical network. Considerable ingenuity and mathematical knowledge have been brought to bear in this area.

The application of Jacobian elliptic functions to the approximation problem originated with Cauer in 1931 (18). He addressed himself

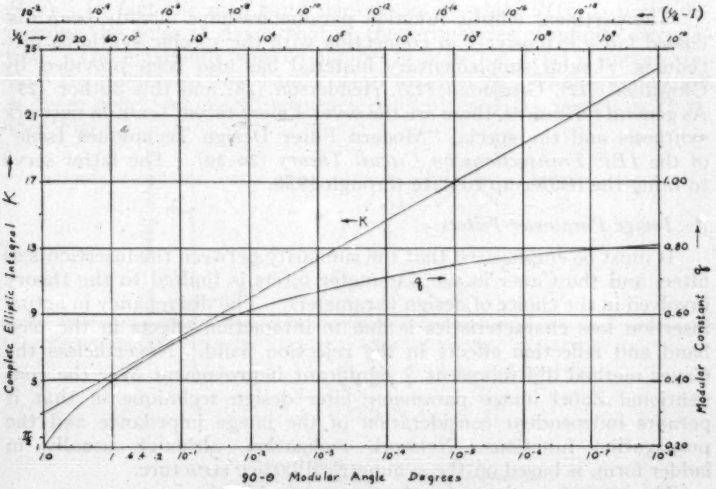

FIG. 3. Elliptic function parameters for extreme values of modular angle.

to the problem of achieving an equiripple, or Tchebycheff, approximation to constant attenuation in the stop band of image parameter filters. Subsequently (1939), they were used to obtain equiripple characteristics in both the pass and stop bands of filters synthesized by the insertion loss theory (19). By then, however, modular transformations were introduced on the elliptic functions to simplify the resulting expressions. These elliptic function approximation methods were also applied (1950) in the design of wide band phase-difference networks (20, 21). Winkler gives a comprehensive survey of the status of this and other approximation techniques as of 1954 (17). Note also the methods given by Papoulis and Deutsch (31, 32).

The key point to observe, for our purposes, is that the elliptic function filters and the phase-difference networks have three distinct frequency bands of interest. The former has equiripple attenuation in the pass and stop bands separated by a monotonic transition region. The latter has the inverse situation, with a prescribed equiripple phase characteristic over a given bandwidth, on either side of which there is a monotonic phase region. This is shown in Fig. 5.

We should note here that the filter discussion is being confined to the low pass case. This involves no loss of generality inasmuch as the usual transformations can be applied to get the high pass, band pass and band stop cases if desired.

3. DESIGN PARAMETERS

The pertinent elliptic function parameters have already been discussed fairly extensively in connection with the specific synthesis procedures. Useful supplementary material has also been provided by Glowatski (22), Grossman (23), Henderson (24) and this author (25). As general references, there are the several more recent texts on network synthesis and the special "Modern Filter Design Techniques Issue" of the *IRE Transactions on Circuit Theory* (26–30). The latter serve to bring the reader up to date through 1958.

A. Image Parameter Filters

It must be emphasized that the similarity between the insertion loss filters and the Cauer image parameter filters is limited to the theory involved in the choice of design parameters. The discrepancy in actual insertion loss characteristics is due to interaction effects in the pass band and reflection effects in the rejection band. Nevertheless the Cauer method did represent a significant improvement over the conventional Zobel image parameter filter design technique in that it permits independent consideration of the image impedance and the propagation functions. Network realization, although usually in ladder form, is based on the symmetrical lattice structure.

The image impedance for the symmetrical lattice is

$$Z_I(\omega) = \pm \sqrt{Z_z(\omega) Z_y(\omega)}. \tag{1}$$

The transfer function, $P_I(\omega)$, can be expressed in terms of a parametric ratio function given by

$$H(\omega) = \pm \sqrt{\frac{Z_z(\omega)}{Z_y(\omega)}}. \tag{2}$$

Then

$$P_I(\omega) = A_I(\omega) + jB_I(\omega)$$
$$= \ln \frac{1 + H(\omega)}{1 - H(\omega)}$$

or alternately as

$$H(\omega) = \tanh \frac{P_{\pi}(\omega)}{2}. \tag{3}$$

The independent parametric relations of Eqs. 1 and 2 determine a purely reactive symmetric lattice. The positive roots are normally used (26).

It is well known that for a low pass filter $Z_I(\omega)$ is controlled by the cutoff frequency ω_c and the stop band critical frequencies, while $H(\omega)$ depends on the cutoff and pass band critical frequencies. It is convenient to use a normalized frequency parameter $x = \omega/\omega_c$. The properties of the transfer loss $A_I(x)$ are intimately related to those of $H(x)$. In fact the stop band frequencies at which $H(x)$ is unity determine the poles of $A_I(x)$, that is, the frequencies of infinite attenuation. The maximum possible number of poles for $A_I(x)$ is one greater than the number of pass band critical frequencies. Thus specification of these poles and cutoff frequency determines $A_I(x)$ as well as $H(x)$. (See Fig. 4.)

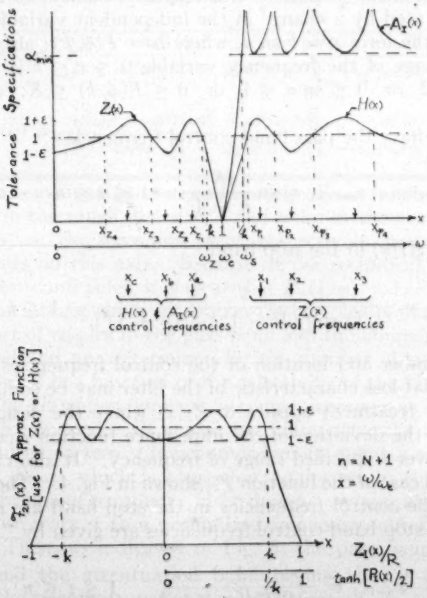

FIG. 4. Data relevant to specification of Cauer image parameter filters.

The information required to start a Cauer parameter filter design is tolerance ϵ, with respect to the minimum value of attenuation α_{min} *versus* the corresponding coverage k. That is the frequency at which α_{min} is first reached. (See Fig. 4.) Then we have

$$\epsilon = \frac{2}{\epsilon^{\alpha_{min}} - 1} = \frac{2}{10^{\alpha_{min}/20} - 1} \tag{4}$$

or its equivalent

$$\alpha_{min} = \ln\left(\frac{2 + \epsilon}{\epsilon}\right).$$

For close tolerance, that is, ϵ small, these can be simplified to $\epsilon = \frac{2}{10^{\alpha_{min}/20}}$ and $\alpha_{min} = \ln \frac{2}{\epsilon}$ respectively. From this it is necessary to determine the number and location of the control frequencies in the pass band.

Location of the control frequencies for Tchebycheff approximation (or geometric mean variation with respect to unity) to a flat transfer loss is facilitated by a change in the independent variable in the $H(x)$ function of the form $x = k \operatorname{sn} u$, where $u = F(\phi, k)$; also, $x = k \sin \phi$. Then the range of the frequency variable $0 \leq x \leq k$ is equivalent to $0 \leq \phi \leq \pi/2$ or $0 \leq \operatorname{sn} u \leq 1$ or $0 \leq F(\phi, k) \leq K$, as shown in Appendix I.

Then we have the pass band control frequencies

$$x_{n+1-i} = \operatorname{sn} \frac{iK}{n+1} \qquad 1 \leq i \leq n \tag{5}$$

and poles of $A_I(x)$ in the stop band

$$x_{p[2(n-i)+3]} = \frac{1}{(1/k) \operatorname{sn} [(2i-1)K/2(n+1)]} \qquad 1 \leq i \leq n+1 \tag{6}$$

Once the number and location of the control frequencies of $A_I(x)$ are known, the flat loss characteristic of the filter may be computed (**26**).

A similar treatment applies to $Z_I(x)$ where the design specifies a tolerance on the deviation of the impedance function $Z(x) = Z_I(x)/R$ from unity over a specified range of frequency. It also can be considered a special case of the function F_{2n} shown in Fig. 4. The number and location of the control frequencies in the stop band are required. In this case the stop band control frequencies are given by

$$x_{n-1-i} = \frac{1}{\operatorname{sn} [iK/(n+1)]} \qquad 1 \leq i \leq n \tag{7}$$

and the unit values of $Z(x)$ on the normalized frequency scale x are given by

$$x_{zi} = k \operatorname{sn} \frac{2(n-i)+3}{2(n-1)} K \qquad 1 \leq i \leq n+1 \tag{8}$$

B. Elliptic Function Filters

On the other hand, for the elliptic function filters, based on insertion loss theory, we start off by letting the required transfer function be a general rational function, given by

$$|Z_{12}|^2 = \frac{1}{1 + h^2 R_n^2(\omega)}. \tag{9}$$

Then the desired filter is specified by any three of the following four parameters: the minimum loss in the stop band, the maximum attenuation in the pass band, the width of the transition region, and the complexity of the function n. This is based on the selection of the appropriate Tchebycheff rational function $R_n(\omega)$ which is of the form

$$R_n(\omega) = \frac{(\omega_1^2 - \omega^2)(\omega_3^2 - \omega^2)\cdots(\omega^2{}_{2n-1} - \omega^2)}{(1 - \omega_1^2\omega^2)(1 - \omega_3^2\omega^2)\cdots(1 - \omega^2{}_{2n-1}\omega^2)}$$

or (10)

$$R_n(\omega) = \frac{\omega(\omega_2^2 - \omega^2)(\omega_4^2 - \omega^2)\cdots(\omega_{2n}^2 - \omega^2)}{(1 - \omega_2^2\omega^2)(1 - \omega_4^2\omega^2)\cdots(1 - \omega_{2n}^2\omega^2)}$$

where the first is even and the second is odd. Each function has zeros on the ω axis in the range $0 < \omega < 1$ and poles in the complementary range $1 < \omega < \infty$, the zeros and poles, respectively, being located at reciprocal points on this axis. Because of the reciprocal relationship between the zeros and poles, it is clear that $R_n(1/\omega) = 1/R_n(\omega)$. Note that here n is an integer which determines the complexity of the function.

The number of ripples in the pass band and the number in the stop band are equal and are determined by the number of poles n. The transition interval is a function of the selectivity of the filter as shown in Fig. 5. The transition interval becomes narrower as functions of higher order n are used. Of course for finite networks this interval cannot be reduced to zero. It is convenient to define a reference frequency, $\omega_0 = \sqrt{\omega_p \omega_a}$, which is somewhat analogous to the cutoff frequency used in image parameter filter design. Again, as a matter of convenience, we work with a normalized frequency variable $\Omega = \omega/\omega_0 = \omega/\sqrt{\omega_p \omega_a}$. Then, as indicated in Fig. 5, the pass band terminates at $\Omega = \sqrt{k}$, and the attentuation band begins at $\Omega = 1/\sqrt{k}$, where $k = \omega_p/\omega_a$ is the selectivity parameter, by definition.

The corresponding insertion power ratio required for a symmetrical filter turns out to be of the form

$$e^{2\alpha} = 1 + (e^{2\alpha_p} - 1)[R(\Omega)]^2 \tag{11}$$

where

$$R(\Omega) = S_0 \frac{\Omega(\Omega^2 - \Omega_1^2)\cdots(\Omega^2 - \Omega_M^2)}{(1 - \Omega_1^2\Omega^2)\cdots(1 - \Omega_M^2\Omega^2)}.$$

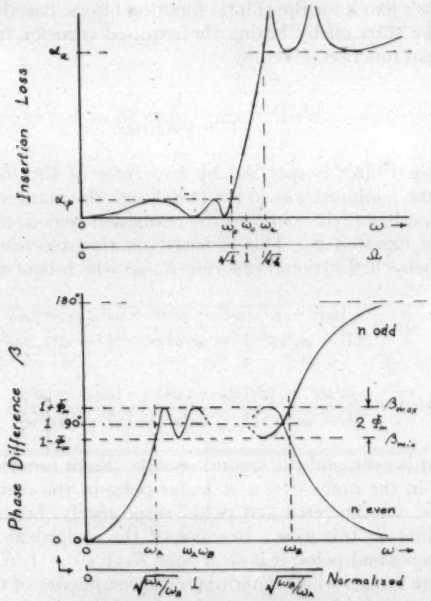

FIG. 5. Typical elliptic function filter and phase-difference network performance curves showing three distinct frequency bands.

The following additional requirements must also be met:

(*a*) $$|R(\Omega)| = \sqrt{(e^{2\alpha_s} - 1)/(e^{2\alpha_p} - 1)} = 1/k_1$$

(*b*) $$S_0 = 1/\sqrt{k_1}$$

(*c*) The selectivity parameter k and the discrimination parameter k_1 are related by the condition $(2M + 1)K'/K = K_1'/K_1$. An alternative expression for this condition is given in terms of modular constants as $q_1 = q^{(2M+1)}$.

(*d*) The frequencies at which the loss is zero and the reciprocal of the frequencies at which the loss is infinite are given by

$$\Omega_s = \sqrt{k}\,\mathrm{sn}\left[\frac{2sK}{2M+1}; k\right] \qquad \begin{matrix} s = 0, 1, 2, \cdots, M \\ \text{and} \\ n = 2M + 1. \end{matrix} \tag{12}$$

In the usual case, the filter design problem consists of the specification of the number of ladder filter sections M required to attain a prescribed minimum band loss α_a, a prescribed transition band $\sqrt{k} \leq \Omega \leq 1/\sqrt{k}$, and a tolerable pass band ripple α_r. The well known expression relating the primary design parameters is

$$\alpha_a \doteq 10[\log (e^{2\alpha_r} - 1) - (2M + 1) \log q] - 12.04 \text{ db}. \tag{13}$$

For additional special design formulas see (**19**, **23**).

C. 90° Phase-Difference Networks

The third type of network involves derivation of two transfer impedances, suitable for all-pass networks, and having approximately $\pi/2$ radians difference between their phase angles over a prescribed band of frequencies. These are usually called 90° phase-difference, or phase-splitting, networks. It can be shown that a suitable rational function where poles and zeros are the negatives of one another can be written as

$$\tan (\Phi/2) = \prod_{j=1}^{n} \left(\frac{\omega_j - \omega}{\omega_j + \omega}\right) \tag{14}$$

where

$$\Phi = \pi/2 - (\beta_1 - \beta_2).$$

This function can be written in terms of parametric equations to give a Tchebycheff approximation to a constant 90° phase difference. Normalizing the prescribed band of frequencies so that the geometric mean of the ends of the band $\sqrt{\omega_A \omega_B}$ equals unity, the parametric equations are:

$$\tan (\Phi/2) = \sqrt{k_1}\,\mathrm{cd}\,[(2nK_1/K)u; k_1] \tag{15}$$

and

$$\omega = 1/\sqrt{k'}\,\mathrm{dn}\,[u; k]. \tag{16}$$

If we express the maximum value of phase difference Φ by Φ_m, we can rewrite Eq. 15 as

$$\tan (\Phi_m/2) = \sqrt{k_1}. \tag{15a}$$

Since $k_1 \ll 1$ normally, we can apply the approximation

$$k_1^2 \approx 16q_1.$$

The corresponding modular constants are related by

$$q_1 = q^{4n}.$$

Then Eq. 15 assumes the alternate form

$$\tan (\Phi_m/2) = 2q^n. \tag{15b}$$

Practical applications are confined to small error angles so that

$$\Phi_m/2 \approx \tan (\Phi_m/2).$$

These approximations result in an equation relating phase tolerance, bandwidth and network complexity.

$$\Phi_m = 4q^n \tag{17}$$

or alternately

$$\Phi_m = 4[\exp (-\pi K'/K)]^n \tag{17a}$$

where

Φ_m = phase-tolerance angle in radians
n = network complexity, that is, the number of first order all-pass sections in network N plus the number in network P. (See Fig. 6.)
q = modular constant or "nome" related to the bandwidth of the network by $\sec \theta = 1/k' = \omega_B/\omega_A$.

Applying some transformations of the elliptic functions to the Eq. 16 we get the necessary equation for determination of the value of the poles and zeros required for all-pass phase-difference network synthesis.

$$p_j = (\omega_B/\omega_A)^{1/2} \frac{cn(u_j; k)}{sn(u_j; k)}$$

$$= (\omega_B/\omega_A)^{1/2} cs(u_j; k) \tag{18}$$

where

$$u_j = \frac{4j + 1}{2n} K$$

and

$$j = 0, 1, 2, \cdots, n - 1.$$

The theoretical sideband rejection attainable by use of these networks can be expressed in terms of a given error angle Φ_m as

$$\text{Rejection } (db) = 20 \log [\cot (\Phi_m/2)]. \tag{19}$$

4. PARAMETER DETERMINATION

In the previous section we summarized the already known fundamental design parameters of the three types of networks being considered. In this section are presented means of relating these parameters involving elliptic functions. This is done in a way which facilitates determination of numerical values while at the same time emphasizing the inherent similarities in concept of these types of networks.

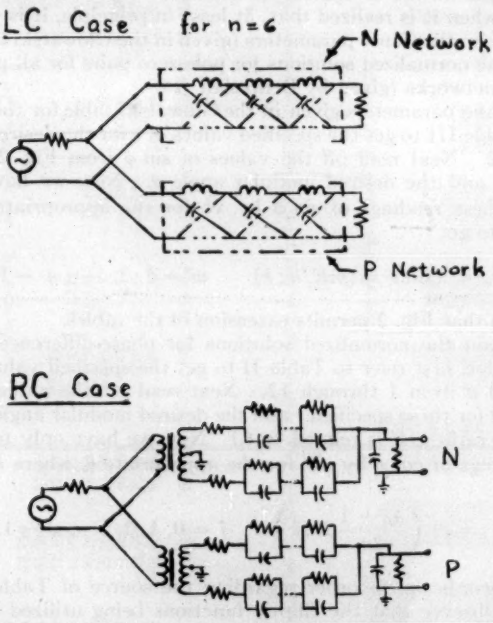

FIG. 6. Phase-difference network configurations.

Specialized representations have been devised by various authors to show the performance capabilities of these networks for various ranges of parameter values including network complexity. Because of the common thread of elliptic functions utilized, however, it becomes possible to use a single representation for all three types at the expense of three sets of scales. This is shown in Fig. 1. If desired the ranges given therein can readily be extended. The alternate representations are also amenable to similar modification.

Similar simplification and consolidation of information are possible

in connection with location of the critical frequencies which are necessary for synthesis of the networks. A family of curves typified by Fig. 2 practically permits determination of these critical frequencies by inspection. An added feature here is that the curves go considerably beyond the usual limitation of modular angle $\theta = 89°$. A tabulation of "amplitude" ϕ to twelve decimal places is available in the Spenceley tables for values of r and θ in integral degrees (10).

The basic nature of the curves shown in Fig. 2 can better be appreciated when it is realized that, at least in principle, it is possible to get from them the Cauer parameters (given in the Glowatski tables (22)) and also the normalized solutions for pole-zero pairs for all-pass phase-difference networks (given by Bedrosian (25)).

To get the parameters given in the Glowatski table for the plot, first refer to Table III to get the specified values of r for the desired n from 1 through 12. Next read off the values of $\sin \phi$ from Fig. 2 for these specified r and the desired modular angle θ. Now we have only to multiply these readings of $\sin \phi$ by $\sqrt{k}$ for the appropriate θ, where $k = \sin \theta$, to get

$$a_m = \sqrt{\sin \theta} \cdot sn(mK/n; k) \qquad m = 1, 2, \cdots, n - 1. \tag{20}$$

Note again that Fig. 2 permits extension of the tables.

To obtain the normalized solutions for phase-difference networks from the plot, first refer to Table II to get the specified values of r for the desired n from 1 through 12. Next read off the values of $\cot \phi$ from Fig. 2 for these specified r and the desired modular angle θ. (The bandwidth ratio $1/k'$ is related to θ.) Now we have only to multiply these readings of $\cot \phi$ by $\sqrt{k'}$ for the appropriate θ, where $k' = \cos \theta$, to get

$$\chi_j = cs\left(\frac{4j + 1}{2n} K; k\right) \qquad j = 0, 1, 2, \cdots, n - 1. \tag{21}$$

A few words are in order regarding the source of Tables II, III, and IV. Observe that the elliptic functions being utilized are of the form $sn(u; k)$, $cs(u; k)$, etc. Furthermore, the variable u is normally given in terms of the complete elliptic integral K which, depending on the elliptic function in question, is a half period or a quarter period of the function. To facilitate the use of the Smithsonian Elliptic Function Table note that the Spenceleys let

$$u = (r/90)K \tag{22}$$

and tabulate it as r (in degrees). In other words the independent variable $u = F(\phi, k)$ is divided into 90° of a quadrant K, that is, into 90 equal steps. In addition to tabulating the usual elliptic functions for

TABLE II.—*Tabulation of Variable* u *in Terms of Angle* r *in Degrees for Phase-Difference Network Application.*

Use with Fig. 2 and Eqs. 18 and 21

n	r											
1	45.000											
2	22.500	−67.500										
3	15.000	−45.000	75.000									
4	11.250	−33.750	56.250	−78.750								
5	9.000	−27.000	45.000	−63.000	81.000							
6	7.500	−22.500	37.500	−52.500	67.500	−82.500						
7	6.429	−19.286	32.143	−45.000	57.857	−70.715	83.572					
8	5.625	−16.875	28.125	−39.375	50.625	−61.875	73.125	−84.375				
9	5.000	−15.000	25.000	−35.000	45.000	−55.000	65.000	−75.000	85.000			
10	4.500	−13.500	22.500	−31.500	40.500	−49.500	58.500	−67.500	76.500	−85.500		
11	4.091	−12.273	20.455	−28.636	36.818	−45.000	53.180	−61.364	69.545	−77.727	85.909	
12	3.750	−11.250	18.750	−26.250	33.750	−41.250	48.750	−56.250	63.750	−71.250	78.750	−86.250
n	$\pi/4n$	$-3\pi/4n$	$5\pi/4n$	$-7\pi/4n$	$9\pi/4n$	$-11\pi/4n$	$13\pi/4n$	$-15\pi/4n$	$17\pi/4n$	$-19\pi/4n$	$21\pi/4n$	$-23\pi/4n$

TABLE III.—*Tabulation of Variable* u *in Terms of Angle* r *in Degrees for Elliptic-Function Filter Application.*

Use with Fig. 2 and Eqs. 12 and 20

n	r											
1	90.000											
2	45.000	90.000										
3	30.000	60.000	90.000									
4	22.500	45.000	67.500	90.000								
5	18.000	36.000	54.000	72.000	90.000							
6	15.000	30.000	45.000	60.000	75.000	90.000						
7	12.857	25.714	38.571	51.428	64.286	77.143	90.000					
8	11.250	22.500	33.750	45.000	56.250	67.500	78.750	90.000				
9	10.000	20.000	30.000	40.000	50.000	60.000	70.000	80.000	90.000			
10	9.000	18.000	27.000	36.000	45.000	54.000	63.000	72.000	81.000	90.000		
11	8.182	16.364	24.506	32.727	40.909	49.091	57.273	65.455	73.638	81.818	90.000	
12	7.500	15.000	22.500	30.000	37.500	45.000	52.500	60.000	67.500	75.000	82.500	90.000
n	$\pi/2n$	$2\pi/2n$	$3\pi/2n$	$4\pi/2n$	$5\pi/2n$	$6\pi/2n$	$7\pi/2n$	$8\pi/2n$	$9\pi/2n$	$10\pi/2n$	$11\pi/2n$	$12\pi/2n$

TABLE IV.—*Tabulation of Variable* u *in Terms of Angle* r *in Degrees for Image Parameter Filter Application.*

(Where $N + 1 = n$, the number of unit values of $H(x)$ or $Z(x)$ and N is the number of control frequencies.)

N	r						
1	45.000						
2	30.000	60.000		Use with Fig. 2 and eqs. 5 and 7			
3	22.500	45.000	67.500	(Note that they are reciprocal)			
4	18.000	36.000	54.000	72.000			
5	15.000	30.000	45.000	60.000	75.000		
6	12.857	25.714	38.571	51.428	64.286	77.143	
7	11.250	22.500	33.750	45.000	56.250	67.500	78.750
N	$\pi/2(N+1)$	$2\pi/2(N+1)$	$3\pi/2(N+1)$	$4\pi/2(N+1)$	$5\pi/2(N+1)$	$6\pi/2(N+1)$	$7\pi/2(N+1)$

N	r						
1	22.500			Use with Fig. 2 and Eqs. 6 and 8			
2	15.000	45.000		(Note that they are basically reciprocal except			
3	11.250	33.750	56.250	for ordering of values obtained)			
4	9.000	27.000	45.000	63.000			
5	7.500	22.500	37.500	52.500	67.500		
6	6.429	19.286	32.143	45.000	57.857	70.715	
7	5.625	16.875	28.125	39.375	50.625	61.875	73.125
N	$\pi/4(N+1)$	$3\pi/4(N+1)$	$5\pi/4(N+1)$	$7\pi/4(N+1)$	$9\pi/4(N+1)$	$11\pi/4(N+1)$	$13\pi/4(N+1)$

$r = 0$ to $r = 90$ for each degree of the modular angle θ (from $\theta = 1$ to $\theta = 89$), they list the corresponding value of ϕ. This ϕ is the amplitude of u. Thus the values of r corresponding to the values of u in the pertinent equations are listed in Tables II, III, and IV.

Finally we consider Fig. 3 which, in conjunction with Table I, permits comparisons of various combinations of the parameters K, θ, k, k', q, etc. as found in the numerous tabulations cited in the Introduction. Here again the range of values presented exceeds that found in the literature. These results should aid the researcher requiring the use of these elliptic parameters at the high values of $\theta \to 90°$ and $k > .999$. For example, the range of the modular constant is $0 \leq q \leq 1$ and of the complete elliptic integrals is $\pi/2 \leq K \leq \infty$. The values given here go up to $q > 0.8$ and $K > 24$. With the choice of scales in Fig. 3, it would be a simple matter to extend the plots as required and still retain the ability to use effective graphical interpolation.

5. CONCLUSIONS

The illustrations given in the preceding sections should be sufficient to demonstrate the important role of elliptic functions in the initial approximation step of network synthesis. The field of application of the tabular and graphical data furnished is by no means limited to the three types of networks discussed. The necessary additional background and detailed discussion of synthesis procedures are beyond the scope of this paper. The insight provided should facilitate understand-

ing and use of the material available in the references. Particular attention is invited to the increasing number of tables of normalized element values useful in meeting practical design problems (30).

APPENDIX I

Elliptic function formulas:

$$u = F(\phi, k) = \int_0^{\phi} \frac{d\psi}{\sqrt{1 - k^2 \sin^2 \psi}} \qquad \text{Elliptic integral of the first kind} \qquad (I\text{-}1)$$

Also

$$u = F(x, k) = \int_0^{x} \frac{dx}{\sqrt{(1 - x^2)(1 - k^2 x^2)}} \qquad (I\text{-}2)$$

where $1 > k > 0$ is the modulus, ϕ is the amplitude of the elliptic integral (that is, $am(u, k)$), and $x = \sin \phi$. When $\phi = \pi/2$ in Eq. I-1:

$$F(\pi/2, k) = K = \int_0^{\pi/2} \frac{d\psi}{\sqrt{1 - k^2 \sin^2 \psi}}. \qquad (I\text{-}3)$$

Similarly if $x = 1$ in Eq. I-2:

$$F(1, k) = K = \int_0^{1} \frac{dx}{\sqrt{(1 - x^2)(1 - k^2 x^2)}}. \qquad (I\text{-}4)$$

There are three basic elliptic functions:

$$sn(u, k) = \sin \phi = x \qquad \text{Odd function} \qquad (I\text{-}5)$$

$$\left.\begin{aligned} cn(u, k) &= \cos \phi = \sqrt{1 - x^2} \qquad (I\text{-}6) \\ dn(u, k) &= \Delta\phi = \sqrt{1 - k^2 x^2} \qquad (I\text{-}7) \end{aligned}\right\} \text{Even functions}$$

Note that these functions are trigonometric functions of ϕ, the amplitude of u. When considered as functions of u they are doubly periodic and are called elliptic functions. The independent variable u is not an angle. It may be real or imaginary as shown in Table V.

TABLE V.—*Periods of the Basic Functions.*

Function	Real Period	Imaginary Period
$sn(u, k)$	$4K$	$2jK'$
$cn(u, k)$	$4K$	$2(K + jK')$
$dn(u, k)$	$2K$	$4jK'$

The analogy to trigonometric functions is further shown by the relations:

$$sn^2 u + cn^2 u = 1 \qquad (I\text{-}8)$$

$$dn^2 u + k^2 sn^2 u = 1. \qquad (I\text{-}9)$$

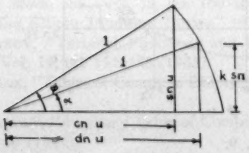

FIG. 7.

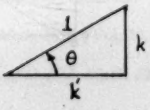

FIG. 8.

Figure 7 shows the interrelations. Recall the limits on the modulus are: $1 > k > 0$. We now define the complementary modulus k'

$$k' = \sqrt{1 - k^2} \quad \text{or} \quad k^2 + k'^2 = 1. \tag{I-10}$$

Also (see Fig. 8)

$$k = \sin\theta \tag{I-11}$$

$$k' = \cos\theta \tag{I-12}$$

where θ = modular angle. (N.B. $\pi/2 - \theta = \phi - \alpha$ in Fig. 8.) Then

$$F(\phi, k') = \int_0^{\phi} \frac{d\psi}{\sqrt{1 - (k')^2 \sin^2\psi}}. \tag{I-13}$$

When $\phi = \pi/2$

$$F(\pi/2, k') = K'. \tag{I-14}$$

Next we define q, the modular constant or "nome"

$$q = \exp(-\pi K'/K). \tag{I-15}$$

This basic number q may also be obtained from the modular angle θ. Graphical representations of these functions for real u are determinable in a simple way from the plots of the elliptic integral as a function of the amplitude. Using Fig. 9, we can get the results shown in Table VI for $\theta = 60°$:

TABLE VI.

u	ϕ	$sn(u, k)$	$cn(u, k)$	$dn(u, k)$
0	0	0	1	1
K	$\pi/2$	1	0	$k' = \frac{1}{2}$
$2K$	π	0	-1	1
$3K$	$3\pi/2$	-1	0	$k' = \frac{1}{2}$
$4K$	2π	0	1	1

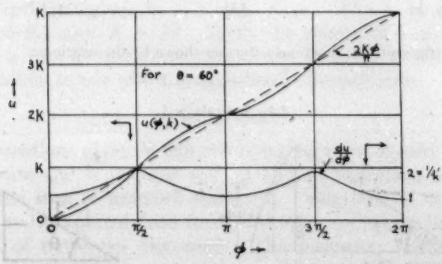

FIG. 9.

APPENDIX II

To get numerical values for the complete elliptic integrals of the first kind $K = F(\pi/2, k)$ and $K' = F(\pi/2, k')$, we offer an alternate form of the series expansion based on the Wallis Theorem (2, 11):

$$K = \frac{\pi}{2}\left[1 + 2\left(\frac{k^2}{8}\right) + 9\left(\frac{k^2}{8}\right)^2 + 50\left(\frac{k^2}{8}\right)^3 + \frac{1225}{4}\left(\frac{k^2}{8}\right)^4 + 2205\left(\frac{k^2}{8}\right)^5 + \cdots\right] \quad \text{for } k^2 \ll 1.$$

For $\theta > 89.95°$, it is simpler to use the expression given by Kaplan (9) to get results with ten-place accuracy:

$$K \approx \left(1 + \frac{k'^2}{4}\right) \ln \frac{4}{k'} - \frac{k'^2}{4}$$

also

$$K' \approx \left(1 + \frac{k^2}{4}\right) \ln \frac{4}{k} - \frac{k^2}{4}.$$

Numerical values of the modular constant q can be obtained by use of the Weierstrass approximation

$$q = d + 2d^5 + 15d^9 + 150d^{13} + 1707d^{17} + 20{,}910d^{21} + 268{,}616d^{25} + \cdots$$

where

$$d = (\tfrac{1}{2})\frac{1 - \sqrt{\cos\theta}}{1 + \sqrt{\cos\theta}} = (\tfrac{1}{2})\frac{1 - \sqrt{k'}}{1 + \sqrt{k'}}$$

The Spenceley tables (10) indicate that this approximation is not good for sixteen-place accuracy for $\theta > 70°$. For larger modular angles we can use:

$$\ln q \ln q' = \pi^2$$

or alternately

$$\log q \log q' = \log \frac{1}{q} \log \frac{1}{q'} = 1.8615228349,$$

where q' is the modular constant of the complementary modulus k'.

REFERENCES

(1) E. T. WITTAKER AND G. N. WATSON, "Modern Analysis," 4th ed., New York, Cambridge University Press, 1940, pp. 429–535.

(2) H. HANCOCK, "Elliptic Integrals," republished by Dover Publications Inc., 1958.

(3) A. EAGLE, "The Elliptic Functions As They Should Be," Cambridge, England, Galloway and Porter, 1958.

(4) A. M. LEGENDRE, "Traite des fonctions elliptique," Tome 2 Paris 1826, pp. 222–243. Tables reprinted in 1931, by F. Emde Stuttgart, and in 1934 by the Biometrika Office, London.

(5) K. HAYASHI, "Taflen der Besselechen, Theta, Kugel und anderer Funktionen," J. Springer, Berlin, 1930. Table of K, pp. 72–81.

(6) L. M. MILNE-THOMPSON, "Ten Figure Table of the Complete Elliptic Integrals," *Proc. London Math. Soc.*, Vol. 33, pp. 160–164 (1930), reprinted by Dover Publications as "Jacobian Elliptic Function Tables," 1950.

(7) J. R. AIREY, "Toroidal Functions and the Complete Elliptic Integrals," *Phil. Mag. Ser. 7*, Vol. 19, pp. 177–188 (1935).

(8) C. HEUMAN, "Tables of Complete Elliptic Integrals," *J. Math. Phys.*, Vol. 20, pp. 127–206 (1941).

(9) E. L. KAPLAN, "Auxiliary Table of Complete Elliptic Integrals," *J. Math. Phys.*, Vol. 25, pp. 26–36 (1946).

(10) G. SPENCELEY AND R. SPENCELEY, "Smithsonian Elliptic Function Tables," Wash. D. C., Smithsonian Institution, Vol. 109, 1947.
(11) E. JAHNKE AND F. EMDE, "Tables of Functions with Formulae and Curves," 4th Ed., reprinted by Dover Publications, Inc., 1945.
(12) M. SCHULER AND H. GEBELEIN, "Acht und neunstellige Tabellen zu den elliptischen Funktionen," Berlin, J. Springer, 1955.
(13) A. R. DIDONATO AND A. V. HERSHEY, "New Formulae for Computing Incomplete Elliptic Integrals of the First and Second Kind," NPG Report No. 1618, NAVORD Report No. 5906; 30 Jan. 1959.
(14) R. G. SELFRIDGE AND J. E. MAXFIELD, "A Table of the Incomplete Elliptic Integral of the Third Kind," New York, Dover Publications Inc., 1959.
(15) H. J. ORCHARD, "Computation of Elliptic Functions of Rational Fractions of a Quarter-period," *IRE Trans. on Circuit Theory*, Vol. CT-5, pp. 352–355 (1958).
(16) L. GOLD, "New Approach to Elliptic Functions," JOUR. FRANKLIN INST., Vol. 267, pp. 503–520 (1959).
(17) S. WINKLER, "The Approximation Problem of Network Synthesis," *IRE Trans. on Circuit Theory*, Vol. CT-1, pp. 5–20 (1954).
(18) W. CAUER, "Theorie der linearen Wechselstromschaltungen," Berlin, Akademie-Verlag, Ger., 2nd ed., 1954. Also in English, "Synthesis of Linear Communication Networks," New York, McGraw-Hill Book Co., 1958.
(19) S. DARLINGTON, "Synthesis of Reactance 4-Poles," *J. Math. Phys.*, Vol. 18, pp. 257–353 (1939).
(20) S. DARLINGTON, "Realization of a Constant Phase Difference," *Bell Sys. Tech. J.*, Vol. 29, pp. 94–104 (1950).
(21) H. J. ORCHARD, "Synthesis of Wideband Two-phase Networks," *Wireless Engineer*, Vol. 27, pp. 72–81 (1950).
(22) E. GLOWATSKI, "Sechstellige Tafel der Cauer-Parameter," Munich, Verlag der Bayerischen Akademie der Wissenchaften, 1955.
(23) A. J. GROSSMAN, "Synthesis of Tchebycheff Parameter Symmetrical Filters," *Proc. IRE*, Vol. 45, pp. 454–473 (1957).
(24) K. W. HENDERSON, "Nomographs for Designing Elliptic Function Filters," *Proc. IRE*, Vol. 46, pp. 1860–1864 (1958).
(25) S. D. BEDROSIAN, "Normalized Design of 90° Phase-Difference Networks," *IRE Trans. on Circuit Theory*, Vol. CT-7, pp. 128–136 (1960).
(26) M. B. REED, "Electric Network Synthesis," Englewood Cliffs, Prentice-Hall, Inc., 1955.
(27) E. A. GUILLEMIN, "Synthesis of Passive Networks," New York, John Wiley & Sons, Inc., 1957.
(28) J. E. STORER, "Passive Network Synthesis," New York, McGraw-Hill Book Co., 1957.
(29) D. F. TUTTLE, JR., "Network Synthesis," Vol. I, New York, John Wiley & Sons, Inc., 1958, Chap. 14.
(30) Modern Filter Design Techniques Issue, *IRE Trans. on Circuit Theory*, Vol. CT-5, (1958).
(31) A. PAPOULIS, "On the Approximation Problem in Filter Design," *IRE National Convention Record*, Vol. 5, Part 2, pp. 175–185 (1957).
(32) S. DEUTSCH, "A Different Approach to the Approximation Problem," *Proc. IRE*, Vol. 48, pp. 1175–1176 (1960).

A METHOD OF DETERMINING PHASE CENTERS AND ITS APPLICATION TO ELECTROMAGNETIC HORNS*

BY

Y. Y. HU[1]

ABSTRACT

A method of locating the phase center of any radiating system from the expression of its radiating field is formulated. This method is then applied to electromagnetic horns of different dimensions and flare angles. It is believed that the results and discussions presented in this paper will be useful in the design and positioning of the feeding horn such that the paraboloidal reflector will produce a desirable radiation pattern.

1. INTRODUCTION

One of the important applications of electromagnetic horns is the use as primary feeds of paraboloidal reflectors. In the usual practice, the relative locations of the horn with respect to the reflector are adjusted by a cut-and-try process until the measured directivity of the radiation pattern is "maximum." It is also known in practice that a "maximum" directive radiation pattern can be obtained if the field distribution on the aperture is equiphase. By the geometry of the paraboloidal reflector, equiphase aperture illumination can be achieved by locating a point source as the primary feed at the focal point. It is apparent that an electromagnetic horn is not a point source, in fact, there is no point source in nature. However, any radiating system is equivalent to a point source within a certain angular region if the equiphase surfaces of its radiation field are concentric spheres in that region. The center of these concentric equiphase spheres is defined as the phase center of this radiating system. In this paper, a method of locating the phase center of any radiating system from the expression of its radiation field is formulated. This method is then applied to electromagnetic horns of different dimensions and flare angles. It is believed that the results presented in this paper will be useful in the design and positioning of the feeding horn such that the paraboloidal reflector will produce a desirable radiation pattern. It is further believed that the method of locating phase center developed here will also be useful in determining the phase center of any other radiator when such information is desired.

* This work was supported in part by Rome Air Development Center, Rome, N. Y., in 1954 under Contract No. AF30(602)-926.

[1] Electrical Engineering Department, Syracuse University, Syracuse, N. Y.

II. A METHOD OF LOCATING PHASE CENTERS

A method of locating the phase center of any radiating system was developed by the author during a study of the phase center of electromagnetic horns (1).[2] For the convenience of presentation, a conical horn is used as an illustration. Referring to Fig. 1, let the coordinate origin be the vertex of the conical horn. If there exists a phase center of the horn, it must be located on the horn axis due to symmetry. The distance from the phase center to the origin is denoted by d which is to be determined. Let the spherical coordinates of any field point P be

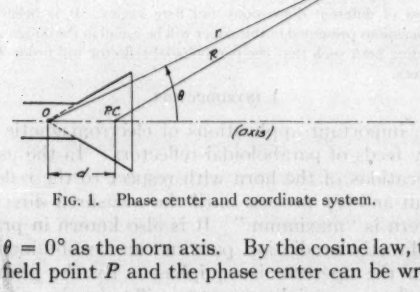

FIG. 1. Phase center and coordinate system.

(r, θ, ϕ) with $\theta = 0°$ as the horn axis. By the cosine law, the distance R between the field point P and the phase center can be written as

$$R = [r^2 + d^2 - 2rd \cos \theta]^{1/2}. \tag{1}$$

The expression is independent upon the azimuth angle ϕ. In the far field, $d \ll r$, Eq. 1 can be approximated by

$$R \cong r - d \cos \theta. \tag{2}$$

The approximate relation (2) can also be obtained by considering distances r and R as parallel lines when P is in the far field.

The field with such a phase center can be expressed as

$$E_p = |M| e^{i\eta} e^{-ikR} \tag{3}$$

where $|M|$ is the amplitude of the field. The phase angle η depends also upon the choice of time reference. Substituting (2) and $k = 2\pi/\lambda$ into Eq. 3, we have

$$E_p = |M| e^{-j2\pi[r/\lambda - (d \cos \theta)/\lambda - \delta]}. \tag{4}$$

[2] The boldface numbers in parentheses refer to the references appended to this paper.

On the other hand, from the theory of electromagnetic radiation, the far field produced by a finite size radiating system can always be expressed in the following form

$$E_p = |M(r, \theta, \phi)| e^{-j[kr - f(\theta, \phi)]}. \quad (5)$$

If the radiating system has a ϕ-symmetry, that is, the radiation field E_p is independent of ϕ, then Eq. 5 can be written simply as

$$E_p = |M(r, \theta)| e^{-j2\pi[r/\lambda - h(\theta)]}. \quad (6)$$

By comparing the two phase factors in Eqs. 4 and 6, it can be concluded that: if the field expressed by Eq. 6 is spherical, then $h(\theta)$, generally, contains two terms, one is $(d \cos \theta)/\lambda$ and the other is a constant δ. The term $(d \cos \theta)/\lambda$ indicates the spherical nature of the wavefront. The constant term δ depends upon the choice of the time reference. By suitable choice of the time reference, δ can be made equal to zero. In the case $\delta = 0$, the ratio $h(\theta)/\cos \theta$ will give the value of d/λ which determines the location of the phase center. A more general way of obtaining d/λ is to plot $h(\theta)$ *versus* $\cos \theta$; it should be a straight line passing through the origin for $\delta = 0$ and its slope is the value d/λ. When $h(\theta)$ contains an additional non-zero value of δ, the plot method can still be used. In such a case, the straight line will not pass through the origin; however, its slope still gives the required d/λ.

Note that the plot of $h(\theta)$ *versus* $\cos \theta$ is a straight line over the entire range of θ ($0° \leq \theta \leq 180°$) only if the radiator is an ideal point source. For a practical radiating system the plot is a straight line only within a certain angular region. Within that angular region, the radiation field is spherical and the location of the phase center, d/λ, is the slope of the straight line part. If no part of the plot is a straight line, then no part of the wave front is spherical, and the concept of phase center is meaningless in such a case.

It is apparent that this method of determining the phase center is very general and can readily be applied to any radiating system with its radiating field expression known. In this paper, the application of this method to sectoral horns (1) only is presented. Besides sectoral horns, this method was later also used to determine the phase centers of helical beam antennas (2, 3).

For a radiating system without a ϕ-symmetry, a single phase center is not defined. However, for any ϕ = constant plane, the phase center can be defined and determined in the same way. The wavefronts in such a plane are simply circular arcs. For sectoral horns, the phase centers in the two principal planes are of practical interest and will be treated in this paper.

III. RADIATION FIELDS OF SECTORAL HORNS

Rectangular horns have been studied in considerable detail in the literature (4–7). The expressions of the radiation fields of sectoral horns have been worked out by Barrow and Chu (4). Their results are derived by using the aperture-diffraction method. In the derivation, the aperture surface is taken to coincide with the cylindrical wavefront of the dominant mode at the mouth of the horn. The aperture field is assumed to be that of the incident wave with the effect of the reflected wave neglected, and the radiation field is then computed by applying the aperture diffraction formula. The field expressions for the E and H sectoral horns in the two principal planes, $\phi = 0°$ and $\phi = 90°$, are listed below in the forms which are convenient for the present applications.

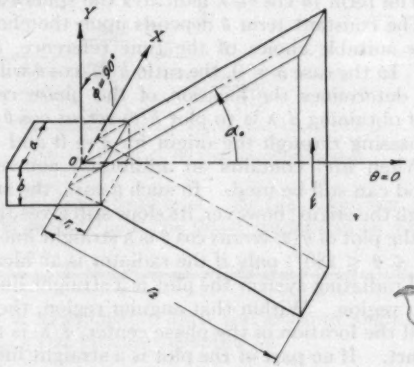

FIG. 2. E-plane sectoral horn.

1. E-Plane Sectoral Horn (Fig. 2)

(a) in the H-plane, $\phi = 0°$ (abbreviated as EH case)

$$E_\phi = A\frac{1}{\pi}\left(\frac{a}{\lambda}\right)\left(\frac{r_2}{r}\right)\frac{\cos\left(\pi\frac{a}{\lambda}\sin\theta\right)}{1-4\frac{a^2}{\lambda^2}\sin^2\theta}\epsilon^{-jkr}\int_{-\alpha_0}^{\alpha_0}\left[jH_1^{(2)}(\beta r_2)\cos\theta + \sqrt{1-\left(\frac{\lambda}{2a}\right)^2}H_0^{(2)}(\beta r_2)\cos\theta'\right]\epsilon^{j2\pi(r_2/\lambda)\cos\theta\cos\theta'}d\theta'$$

(b) in the E-plane, $\phi = 90°$ (abbreviated as EE case)

$$E_\theta = -A\frac{1}{\pi}\left(\frac{a}{\lambda}\right)\left(\frac{r_2}{r}\right)e^{-jkr}\int_{-\alpha_0}^{\alpha_0}\left[jH_1^{(2)}(\beta r_2) + \sqrt{1-\left(\frac{\lambda}{2a}\right)^2}H_0^{(2)}(\beta r_2)\cos(\theta-\theta')\right]\epsilon^{j2\pi(r_1/\lambda)\cos(\theta-\theta')}d\theta'. \quad (8)$$

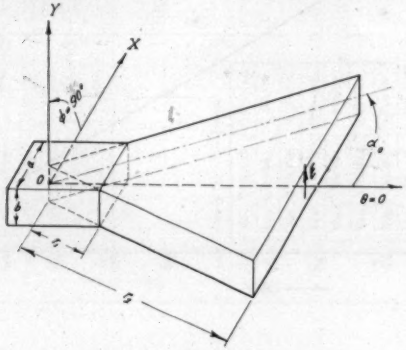

FIG. 3. H-plane sectoral horn.

2. H-plane Sectoral Horn (Fig. 3)

(a) in the H-plane, $\phi = 0°$ (abbreviated as HH case)

$$E_\phi = Aj\frac{1}{2\lambda}\frac{b}{r}\frac{r_2}{r}\epsilon^{-jkr}\int_{-\alpha_0}^{\alpha_0}\left[H_0^{(2)}\left(2\pi\frac{r_2}{\lambda}\right)(\cos p\theta')\cos(\theta-\theta') + jH_p^{(2)\prime}\left(2\pi\frac{r_2}{\lambda}\right)(\cos p\theta')\right]\epsilon^{j2\pi(r_1/\lambda)\cos(\theta-\theta')}d\theta'. \quad (9)$$

(b) in the E-plane, $\phi = 90°$ (abbreviated as HE case)

$$E_\theta = Aj\frac{1}{2\pi}\frac{r_2}{r}\frac{\sin\left(\pi\frac{b}{\lambda}\sin\theta\right)}{\sin\theta}\epsilon^{-jkr}\int_{-\alpha_0}^{\alpha_0}\left[H_p^{(2)}\left(2\pi\frac{r_2}{\lambda}\right)(\cos p\theta')\cos\theta' + jH_p^{(2)\prime}\left(2\pi\frac{r_2}{\lambda}\right)\cos\theta\,(\cos p\theta')\right]\epsilon^{j2\pi(r_1/\lambda)\cos\theta\cos\theta'}d\theta', \quad (10)$$

where $p = \pi/2\alpha_0$ and $H_p^{(2)}$ is the Hankel's function of the second kind and p^{th} order. The meaning of the remaining symbols appears in Fig. 2 or Fig. 3.

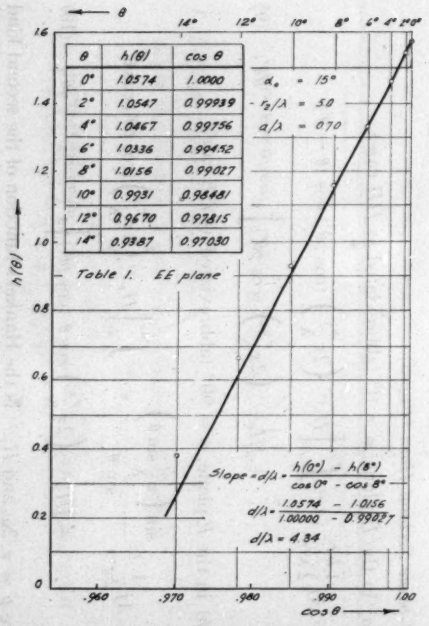

FIG. 4. Illustration for determining d/λ from the plot of $h(\theta)$ *versus* cos θ (*EE*p lane).

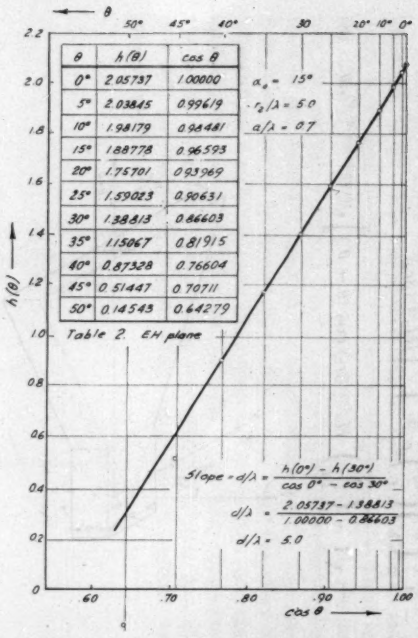

FIG. 5. Illustration for determining d/λ from the plot of $h(\theta)$ *versus* cos θ (*EH* plane).

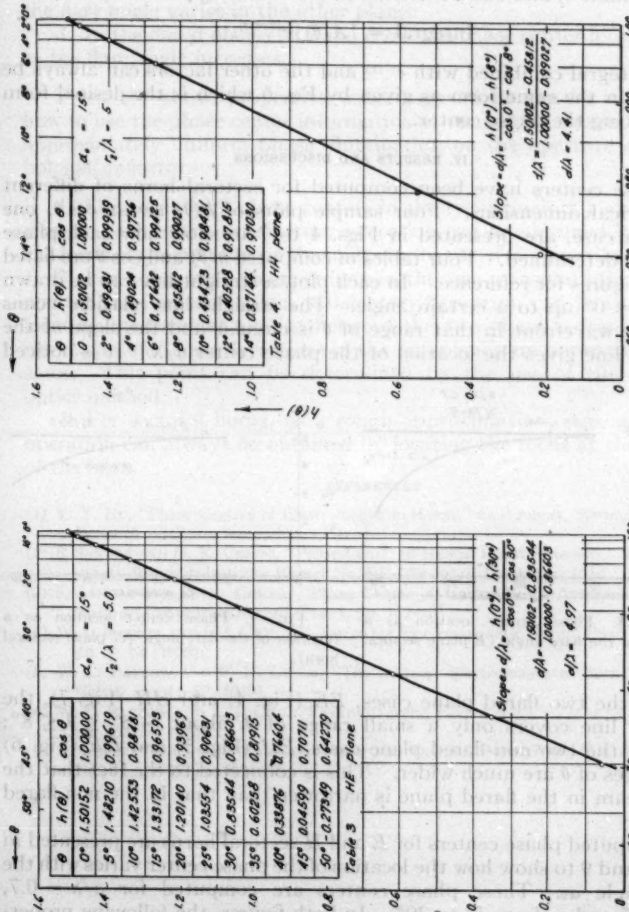

FIG. 7. Illustration for determining d/λ from the plot of $h(\theta)$ *versus* $\cos\theta$ (*HH* plane).

FIG. 6. Illustration for determining d/λ from the plot of $h(\theta)$ *versus* $\cos\theta$ (*HE* plane).

All the integrals in Eqs. 7, 8, 9 and 10 are complex functions of a real variable θ, and can be written in the following polar form.

$$\text{Integral} = |A(\theta)|e^{j2\pi h(\theta)}.$$

Each integral combined with e^{-jkr} and the other factors can always be written in the same form as given by Eq. 6 which is the desired form for locating the phase center.

IV. RESULTS AND DISCUSSIONS

Phase centers have been computed for sectoral horns of different geometrical dimensions. Four sample plots of $h(\theta)$ *versus* $\cos\theta$, one for each case, are presented in Figs. 4 to 7 to show how each phase center is determined. Four tables of computed $h(\theta)$ and $\cos\theta$ are listed on the figures for reference. In each plot, a straight line can be drawn from $\theta = 0°$ up to a certain angle. The straight line relation means that the wavefront in that range of θ is circular and the slope of the straight line gives the location of the phase center d/λ. It is noticed

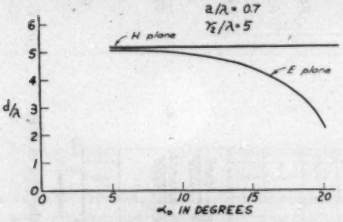

FIG. 8. Phase center location as a function of the flare angle (E plane sectoral horn).

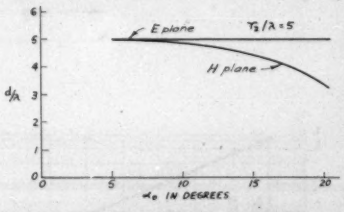

FIG. 9. Phase center location as a function of the flare angle (H plane sectoral horn).

that in the two flared plane cases, EE (Fig. 4) and HH (Fig. 7), the straight line covers only a small range of θ, about $-8° \leq \theta \leq 8°$; while in the two non-flared plane cases, EH (Fig. 5) and HE (Fig. 6) the ranges of θ are much wider. This is connected to the fact that the main beam in the flared plane is narrower than that in the non-flared plane.

Computed phase centers for E and H sectoral horns are presented in Figs. 8 and 9 to show how the location of the phase center varies with the flare angle α_0. These phase centers are computed for $a/\lambda = 0.7$, $r_2/\lambda = 5$ and α_0 from 5° to 20°. In both figures, the following properties are observed.

1. At small flare angles, the phase centers in the E-plane and H-plane almost coincide. They deviate from each other as the flare angle increases.

2. In the non-flared planes (*EH* and *HE*), the phase center remains almost fixed and is located close to the aperture of the horn even when the flare angle varies in the other plane.

3. In the flared planes (*EE* and *HH*), the phase center moves inward as the flare angle increases.

From the above properties, some suggestions can be made about how to use the phase center information of sectional horns in producing approximately uniform phase illumination on the aperture of a paraboloidal reflector.

1. For horns with phase centers in the two principal planes located close to each other, satisfactory operation can be obtained by locating the focus of the reflector at the midpoint between the two phase centers.

2. For horns with phase centers in the two principal planes located not too close to each other, satisfactory operation can be obtained by locating the focus at a point between the two phase centers such that the maximum phase deviations in the two planes are approximately the same. This point can be determined by the use of the geometric optics method.

3. For sectoral horns, as a rough approximation, reasonably good operation can always be obtained by locating the focus at the aperture of the horn.

REFERENCES

(1) Y. Y. Hu, "Phase Centers of Electromagnetic Horns," final report, Syracuse University Research Institute, September, 1954.

(2) S. Sander and D. K. Cheng, "Phase Center of Helical Beam Antennas," Syracuse University Research Institute Report No. EE 393–5612I, December, 1956.

(3) S. Sander and D. K. Cheng, "Phase Center of Helical Beam Antennas," 1958 IRE National Convention Record, Part I, pp. 152–157.

(4) W. L. Barrow and L. J. Chu, "Theory of the Electromagnetic Horn," *Proc. IRE*, Vol. 27, pp. 51–64 (1939).

(5) W. L. Barrow and F. D. Lewis, "The Sectoral Electromagnetic Horn," *Proc. IRE*, Vol. 27, pp. 41–50 (1939).

(6) W. L. Barrow and L. J. Chu, "Electromagnetic Horn Design," *Trans. AIEE*, Vol. 58, pp. 333–337 (1939).

(7) S. Silver, "Microwave Antenna Theory and Design," New York, McGraw-Hill Book Co., Inc., 1949, pp. 349–358.

CREEP ANALYSIS OF ROTATING SOLID DISKS WITH VARIABLE THICKNESS AND TEMPERATURE

BY

B. M. MA[1]

SUMMARY

A creep analysis for stress distributions in rotating solid disks of variable thickness and variable temperature is presented. This analysis is based on the theory of the Tresca criterion and the associated flow rule. The chief advantage of this analysis for stress distribution is that the complicated problem of disk design in gas turbines and jet engines can be solved with great simplicity by the closed form. The results obtained for the disk design will be on the conservative side.

In this paper, the exponential function creep law at steady-state conditions will be employed. The profile of the meridian section of the disk is assumed to be of the hyperbolic form, and the temperature variation and the creep-rate distribution are assumed to be power functions of the radius of the disk. Some examples will be worked out for calculating the theoretical stress distributions in variable thickness and variable temperature disks. Stress distributions in uniform-thickness and variable-temperature disks will also be given for the purpose of comparison.

NOMENCLATURE

The following nomenclature is used in the paper:

c, c_1, l, m, K = constant
$h = f(r) = cr^m = cr_o^m x^m = h_o x^m$ = thickness of disk
λ = a multiplier or a parameter which is a function of x
r = radius to any point of disk
r_i = inner radius of disk
r_o = outer radius of disk
r_e = radius to the point x_e of disk
t = time
T = absolute temperature
$\dot{u}$ = rate of radial displacement of disk at radius r
$x = r/r_o$
$x_i = r_i/r_o$
$x_c = r_c/r_o$
x_m = the point at which σ_t and σ_r are maximum
σ = equivalent or effective stress
$\sigma_a = \rho\omega r_o^2$ = equivalent inertial stress in rotating thin ring of radius r_o
σ_0 = material creep modulus, having dimensions of stress
σ_t, σ_r, σ_z = tangential, radial and axial stresses of disk, respectively
σ_{r_o} = radial stress at r_o of disk
σ_{r_e} = radial stress at x_e
σ_{t_e} = tangential stress at x_e
σ_{t_m}, σ_{r_m} = maximum tangential and radial stresses, respectively
$\dot{\epsilon}$ = creep rate or effective creep rate

[1] Department of Mechanical Engineering, South Dakota State College, Brookings, S. D.; currently on leave of absence and with the Department of Mechanical Engineering, University of Michigan, Ann Arbor, Mich.

$\dot{\epsilon}_t, \dot{\epsilon}_r, \dot{\epsilon}_z$ = tangential, radial and axial creep rates of disk, respectively
$\epsilon_t, \epsilon_r, \epsilon_z$ = tangential, radial and axial creep strains of disk, respectively
$\rho = \gamma/g$ = density of disk material
γ = specific weight of disk material
g = gravitational acceleration
ω = angular speed of disk

1. INTRODUCTION

This paper may be considered an extension of the previous paper (1)[2] in which some formulas were derived for creep strains and stress analysis in rotating solid disks of variable thickness and uniform temperature. In the previous paper the temperature variation from the rim to the center of gas-turbine and jet-engine disks was not taken into consideration. Consequently, the mathematical derivations of the strain and stress formulas were less involved.

Actually, the disk itself carries the turbine blades. Both the blade roots and the rim of the disk are highly heated by contact with hot gases and by conduction from the turbine blades. Consequently, higher temperatures and steeper thermal gradients are developed in these parts than those near the central portion of the disk. At the same time, the creep effects are cumulative near the periphery of the disk. Therefore, the combine factors of relatively high temperatures, steep thermal gradients and cumulative creep effects will usually cause the creep of the disk to be most severe where the blade roots are held.

Since the rotating disks of gas turbines and jet engines are operated under high temperatures and high speeds, the centrifugal forces may produce stresses that exceed the yield strength of the disk material with the result that plastic flow is produced.

The interaction of this plastic flow and creep, together with the variation of thermal gradients at high temperatures in the disk, may cause further serious stress distributions and even failures that might not be predicted on the basis of purely elastic- or plastic-stress analysis.

In this paper, the stress analysis of rotating solid disks having variable thickness and variable temperature will be presented. This analysis will be based on the theory of the Tresca criterion and its associated flow rule, and will use the exponential function creep law at steady-state conditions. Examples which illustrate the application of the theoretical analysis for stress distributions in the disk will also be given.

In general, the stress distributions in the disk may be divided into the following two regions:[3]

(1) $\sigma_t > \sigma_r > \sigma_z = 0, x_e \leq x \leq 1$ for the outer region of the disk

(2) $\sigma_t = \sigma_r > \sigma_z = 0, x_i \leq x \leq x_e$ for the inner region of the disk

[2] The boldface numbers in parentheses refer to the references appended to this paper.
[3] The symbols used in this paper are defined in the Nomenclature Section on pp. 1–2.

It should be noted that in the inner region of the disk the pattern of stress distribution is identical to that in the disk of uniform strength, namely $\sigma_t = \sigma_r =$ constant.

A solid disk of uniform strength which may be called the exponential disk is suitable for relatively higher peripheral velocities, σ_{r_0}/σ_a, (when the material and outside radius of the disk are given) of high-speed gas turbines and jet engines. It may be noted that the hyperbolic disk assumed in the present paper gives the same pattern of stress distribution in the most-stressed region of the disk as the disk of uniform strength, but has the advantage of less mathematical involvement than the exponential disk.

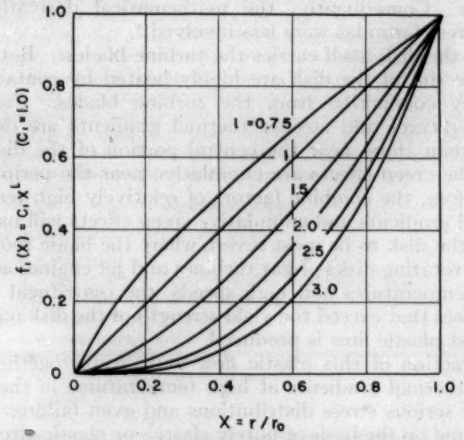

FIG. 1. Temperature distributions in rotating solid disk.

2. THE BASIC EQUATIONS

As discussed in a previous paper (2), the creep rate, $\dot{\epsilon}$, is assumed to be equal to the product of a function of effective stress, $F(\sigma)$, a function of time, $f(t)$, and a function of temperature, $g(T)$, that is,

$$\dot{\epsilon} = F(\sigma)f(t)g(T). \tag{1}$$

It is further assumed that the function of effective stress, $F(\sigma)$, may take the form of the exponential function creep law, e^{σ/σ_0}, for relatively high stresses or high temperatures. Where σ is the effective or equivalent stress in the maximum shear theory and σ_0 the material creep modulus. As to the function of temperature, $g(T)$, in taking the temperature variations into account, we further postulate that the temperature varies with a power function of the radius r or x of the disk (3),

and the creep rate likewise increases with the power function of x at the steady-state condition, provided that $F(\sigma)$ remains unchanged. Hence

$$g(T) = g[f(x)] = f_1(x) = c_1 x^l \tag{2}$$

and

$$\dot{\epsilon} = F(\sigma) f(t) f_1(x) \tag{1a}$$

where c_1 and l are constants. The function $f_1(x)$ for the various values of l and x ($c_1 = 1$) is plotted in Fig. 1.

Based on the foregoing discussion, the basic assumptions given in the previous paper (1), and the associated flow rule of Tresca (4), Eq. 1a for the problem of disks may be written as follows:

$$\left.\begin{aligned} \dot{\epsilon}_t &= -\dot{\epsilon}_z = \frac{\dot{u}}{r_o x} = K e^{\sigma_t/\sigma_o} f(t) f_1(x) \\ \dot{\epsilon}_r &= \frac{\partial \dot{u}}{r_o \partial x} = 0 \end{aligned}\right\} \tag{3}$$

for $\sigma_t > \sigma_r > 0$ and $x_c \leq x \leq 1$; and

$$\left.\begin{aligned} \dot{\epsilon}_t &= \frac{\dot{u}}{r_o x} = \lambda K e^{\sigma_t/\sigma_o} f(t) f_1(x) \\ \dot{\epsilon}_r &= \frac{\partial \dot{u}}{r_o \partial x} = (1 - \lambda) K e^{\sigma_t/\sigma_o} f(t) f_1(x) \\ \dot{\epsilon}_z &= -(\dot{\epsilon}_t + \dot{\epsilon}_r) = -K e^{\sigma_t/\sigma_o} f(t) f_1(x) \end{aligned}\right\} \tag{4}$$

for $\sigma_t = \sigma_r > 0$, $x_i \leq x \leq x_c$ and $\frac{1}{2} \leq \lambda \leq 1$; where λ is a multiplier or a parameter which is a function of x. Here the incompressibility equation, $\dot{\epsilon}_t + \dot{\epsilon}_r + \dot{\epsilon}_z = 0$, has been used in Eqs. 3 and 4.

Integrating Eqs. 3 and 4, the basic equations for creep strains are obtained.

$$\left.\begin{aligned} \epsilon_t &= -\epsilon_z = K e^{\sigma_t/\sigma_o} f_1(x) \left[\int_0^t f(t)dt\right] \\ \epsilon_r &= 0 \end{aligned}\right\} \tag{5}$$

for $\sigma_t > \sigma_r > 0$, $x_c \leq x \leq 1$; and

$$\left.\begin{aligned} \epsilon_t &= \lambda K e^{\sigma_t/\sigma_o} f_1(x) \int_0^t f(t)dt \\ \epsilon_r &= (1 - \lambda) K e^{\sigma_t/\sigma_o} f_1(x) \int_0^t f(t)dt \\ \epsilon_z &= -(\epsilon_t + \epsilon_r) = -K e^{\sigma_t/\sigma_o} f_1(x) \int_0^t f(t)dt \end{aligned}\right\} \tag{6}$$

for $\sigma_t = \sigma_r > 0$, $x_i \leq x \leq x_o$ and $\frac{1}{2} \leq \lambda \leq 1$. The initial creep strains have been assumed to be zero. It should be also noted that at the steady-state condition the effective stress is independent of the time.

The well-known equilibrium equation for the element at radius r or x of the rotating disk, Fig. 2, is given by

$$d(hx\sigma_r)/dx - h\sigma_t + \sigma_a h x^2 = 0 \tag{7}$$

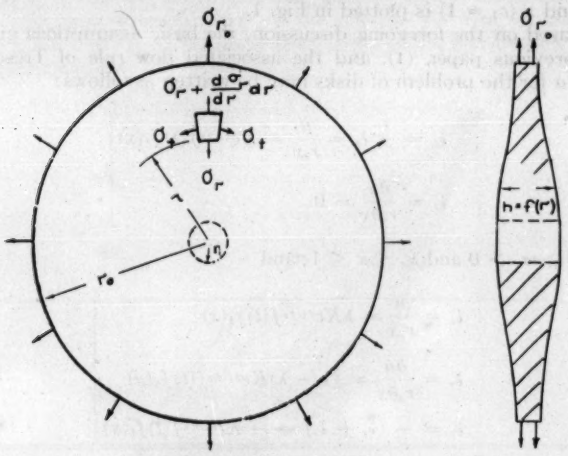

FIG. 2. Rotating solid disk.

in which h is the variable thickness of the disk and $\sigma_a = \rho\omega^2 r_o^2$, the equivalent inertial stress in rotating thin ring of radius r_o.

In order to determine the stresses σ_t and σ_r, it is necessary to introduce one more independent equation in addition to the equilibrium equation. This is the equation of compatibility since the disk is one of the redundant structures.

Thus the known compatibility equation for creep rate of the disk may be simply given by

$$\frac{\partial}{\partial x}(x\dot{\epsilon}_t) - \dot{\epsilon}_r = 0. \tag{8}$$

3. DERIVATIONS FOR THE STRESS EQUATIONS OF CREEP

1. Outer Region of the Disk

Substituting Eqs. 3 into Eq. 8 and simplifying, we have

$$\frac{1}{x} + \frac{1}{\sigma_o}\frac{d\sigma_t}{dx} + \frac{df_1}{f_1 dx} = 0.$$

Upon integration between x_c and x, this yields in the non-dimensional form

$$\frac{\sigma_t}{\sigma_a} = \frac{\sigma_{t_c}}{\sigma_a} + \frac{\sigma_o}{\sigma_a} \ln \frac{x_c f_1(x_c)}{x f_1(x)} \tag{9}$$

in which σ_{t_c} is the tangential stress at $x = x_c$. Now introducing Eq. 9 into Eq. 7 and integrating between x_c and x, the expression for the radial stress is obtained.

$$\frac{\sigma_r}{\sigma_a} = \frac{1}{hx}\left[\int_{x_c}^{x} \left\{ \frac{\sigma_{t_c}}{\sigma_a} + \frac{\sigma_o}{\sigma_a} \ln \frac{x_c f_1(x_c)}{x f_1(x)} \right\} h dx - \int_{x_c}^{x} hx^2 dx + h_c x_c \frac{\sigma_{t_c}}{\sigma_a}\right] \tag{10}$$

where $\sigma_{r_c} = \sigma_{t_c}$ at the point $x = x_c$. Now if we let $x = 1$ and $\sigma_r = \sigma_{r_o}$ at the outside radius of the disk r_o, and then substitute these values into Eq. 10 and rearrange, the following equation for stress at x_c is found.

$$\frac{\sigma_{t_c}}{\sigma_a} = \frac{\sigma_{r_c}}{\sigma_a} = \left[\frac{h_o \sigma_{r_o}}{\sigma_a} - \frac{\sigma_o}{\sigma_a} \int_{x_c}^{1} \ln \frac{x_c f_1(x_c)}{x f_1(x)} h dx + \int_{x_c}^{1} hx^2 dx \right] \Big/ \left(h_c x_c + \int_{x_c}^{1} h dx \right). \tag{11}$$

Upon substitution of the values $h = cr_o^m x^m = h_o x^m$ for the hyperbolic profile of the disk (c and m are constant but m is a negative value), and $f_1(x) = c_1 x^l$, $f_1(x_c) = c x_c^l$ for the temperature or creep-rate distributions in the disk. Equations 9, 10 and 11 for $x_c \leq x \leq 1$ may become, respectively,

$$\frac{\sigma_t}{\sigma_a} = \frac{\sigma_{t_c}}{\sigma_a} + \frac{\sigma_o}{\sigma_a}(1+l) \ln \frac{x_c}{x} \tag{9a}$$

$$\frac{\sigma_r}{\sigma_a} = \frac{1}{x^{1+m}}\left[\frac{x^{1+m} + m x_c^{1+m}}{1+m} \frac{\sigma_{t_c}}{\sigma_a} - \frac{1+l}{1+m}\left(x^{1+m} \ln \frac{x}{x_c} - \frac{x^{1+m} - x_c^{1+m}}{1+m} \right) \frac{\sigma_o}{\sigma_a} - \frac{x^{3+m} - x_c^{3+m}}{3+m} \right] \tag{10a}$$

$$\frac{\sigma_{t_c}}{\sigma_a} = \frac{\sigma_{r_c}}{\sigma_a} = \frac{1+m}{1+m x_c^{1+m}} \left[\frac{\sigma_{r_o}}{\sigma_a} - \frac{\sigma_o}{\sigma_a} \frac{1+l}{1+m} \left(\ln x_c + \frac{1-x_c^{1+m}}{1+m} \right) + \frac{1-x_c^{3+m}}{3+m} \right]. \tag{11a}$$

It can be readily verified that at $x = x_c$, Eqs. 9a and 10a reduce identically to $\sigma_{t_c} = \sigma_{r_o}$, which can be determined from Eq. 11a when the values of l, m, x_c, σ_o/σ_a and σ_{r_o}/σ_a are prescribed. It is also noted that for the particular case when $x_c = 1$, Eq. 11a reduces to $\sigma_{t_c} = \sigma_{r_o} = \sigma_{r_o}$ at r_o.

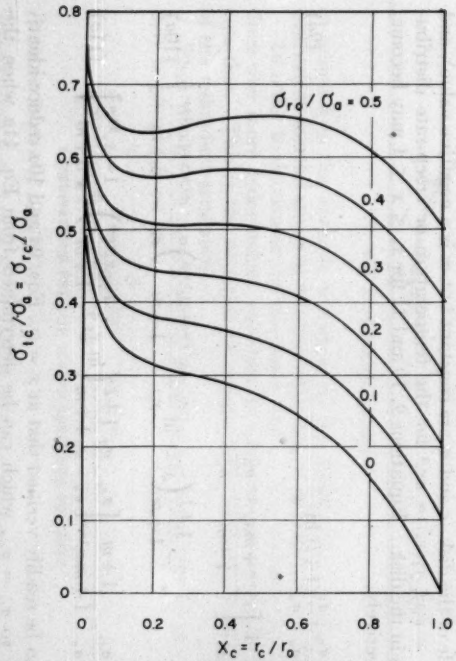

FIG. 3. Creep stresses at different values of x_c, $l = 1.5$, $m = -0.5$, $\sigma_o/\sigma_a = 0.0275$.

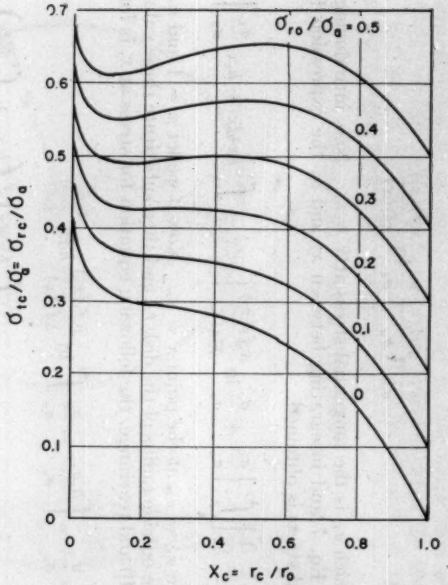

FIG. 4. Creep stresses at different values of x_c, $l = 2.5$, $m = -0.5$, $\sigma_o/\sigma_a = 0.0275$.

Now if we assume values of $l = 1.5$ and 2.5, $m = -\frac{1}{2}$, $r_o = 10$ in. and $\sigma_o/\sigma_a = 0.0275$ (this corresponds to the case where $\sigma_o = 7{,}000$ psi., $\sigma_a = 254{,}500$ psi. at a disk speed of 17,800 rpm., and $\gamma = 0.283$ lb. per cu. in.) and substitute these values in Eq. 11*a*, the resulting values of σ_{t_c}/σ_a plotted against x_c for various values of σ_{r_o}/σ_a will be as shown in Figs. 3 and 4.

Either the inertial radial stress of the disk, σ_{r_o}, or the total centrifugal force of the turbine buckets or blades, that is transmitted through the rim of the disk to the disk proper, can be approximately calculated for any given dimensions of the disk and blades. To calculate this, we may integrate the elemental centrifugal forces from the tip to the root of the blades. In addition, the centrifugal force due to the rim of the disk may be also included.

In order to determine the critical value of x $(=x_c)$ at which the condition $\sigma_t > \sigma_r > 0$ will not be satisfied, we divide Eq. 10*a* by Eq. 9*a*; differentiate the ratio σ_r/σ_t with respect to x and put it equal to zero for a maximum at $x = x_c$. This results in

$$x_c = \left[\frac{1}{\sigma_a}\{\sigma_o(1 + l) - m\sigma_{t_c}\}\right]^{1/2} \qquad \text{(take the positive sign).} \quad (12)$$

With the given values of l, m, σ_o/σ_a and σ_{t_c}/σ_a as calculated from Eq. 11*a* or selected from Fig. 3 or 4, the critical value of x_c can be readily found. Take for example, $l = 1.5$, $m = -\frac{1}{2}$, $\sigma_{r_o}/\sigma_a = 0.4$ (the largest value of σ_{r_o}/σ_a to be assumed in the later examples) and $\sigma_{t_c}/\sigma_a = 0.568$ from Fig. 3. The resulting critical value of x_c as calculated from Eq. 12 (using the above values of l, m, σ_{t_c}/σ_a and $\sigma_o/\sigma_a = 0.0275$) is 0.595. In this particular case, any assumed value of x_c less than the calculated value of 0.595 will not satisfy the required condition $\sigma_t > \sigma_r > 0$, over a portion of the outer region of the disk. This is the reason why the value of x_c will be assumed to be 0.60 or larger in the curves shown in Figs. 5 and 6.

2. Inner Region of the Disk

In this region, since $\sigma_t = \sigma_r$, Eq. 7 can be simply integrated between x and x_c, we have

$$\frac{\sigma_t}{\sigma_a} = \frac{\sigma_r}{\sigma_a} = \frac{1}{h}\left[h_c\frac{\sigma_{t_c}}{\sigma_a} + \int_x^{x_c} hx\,dx\right]. \quad (13)$$

Introducing the thickness function $h = h_o x^m$ and $h_c = h_o x_c^m$, now we have

$$\frac{\sigma_{t_c}}{\sigma_a} = \frac{\sigma_{r_c}}{\sigma_a} = \left(\frac{x_c}{x}\right)^m\frac{\sigma_{t_c}}{\sigma_a} + \frac{x_c^{2+m} - x^{2+m}}{(2 + m)x^m} \qquad x_i \le x \le x_c. \quad (13a)$$

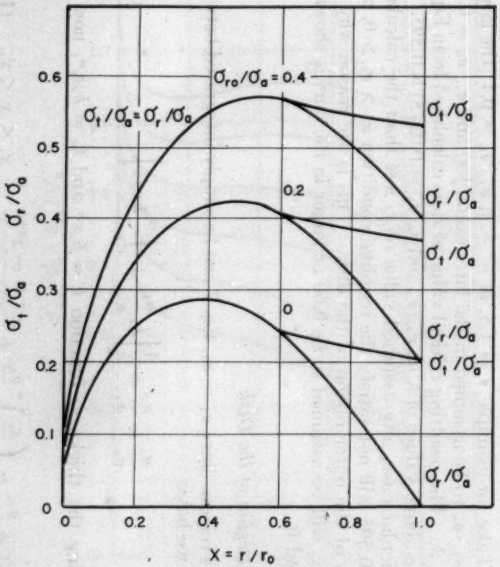

FIG. 5. Creep stresses in rotating solid disk, $l = 1.5$, $m = -0.5$, $x_c = 0.6$.

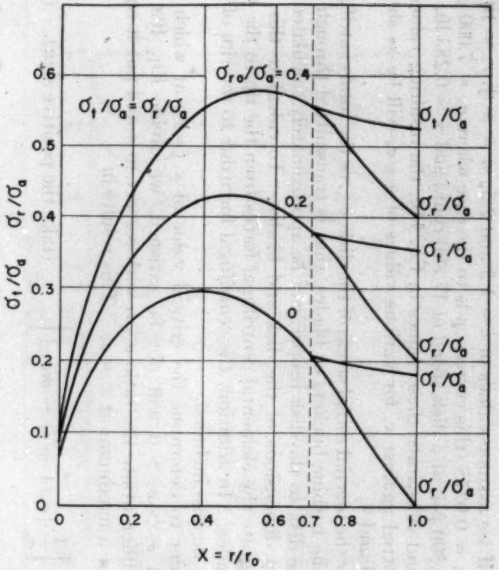

FIG. 6. Creep stresses in rotating solid disk, $l = 1.5$, $m = -0.5$, $x_c = 0.7$,

To find the maximum or peak stresses in the disk, which is of most interest in practical design, we differentiate Eq. 13*a* with respect to x, set it equal to zero and solve for $x = x_m$ where the maximum stresses occur. This gives

$$x_m = \left[-\frac{m(2+m)}{2} \left(\frac{\sigma_{t_c}}{\sigma_a} x_c^m + \frac{x_c^{2+m}}{2+m} \right) \right]^{1/(2+m)} \tag{14}$$

$$\frac{\sigma_{t_m}}{\sigma_a} = \frac{\sigma_{r_m}}{\sigma_a} = \left(\frac{x_c}{x_m} \right)^m \frac{\sigma_{t_c}}{\sigma_a} + \frac{x_c^{2+m} - x_m^{2+m}}{(2+m)x_m^m}. \tag{15}$$

In order to determine the value of λ if it satisfies the condition $\frac{1}{2} \leq \lambda \leq 1$ for $x_i \leq x \leq x_c$, we now substitute Eqs. 4 into Eq. 8, differentiate and rearrange. Thus

$$\frac{d\lambda}{dx} + \left(\frac{1}{\sigma_a} \frac{d\sigma_t}{dx} + \frac{df_1}{f_1 dx} + \frac{2}{x} \right) \lambda = \frac{1}{x}.$$

Using $f_1 = f_1(x) = cx^l$, integrating this equation between x and x_c, and taking $\lambda = 1$ at $x = x_c$, we obtain

$$\lambda = \left(\frac{x_c}{x} \right)^{2+l} e^{(\sigma_{t_c} - \sigma_t)/\sigma_a} - e^{-\sigma_t/\sigma_a} \frac{1}{x^{2+l}} \int_x^{x_c} e^{\sigma_t/\sigma_a} x^{1+l} dx \tag{16}$$

in which σ_{t_c} is given by Eq. 11*a* and σ_t is given by Eq. 13*a*. By a numerical evaluation of the integral in Eq. 16, it may be found whether or not the condition $\frac{1}{2} \leq \lambda \leq 1$ holds for $x_i \leq x \leq x_c$. Experience shows that this is usually true.

The procedure for stress analysis in rotating solid disks of variable thickness and variable temperature may be summed up as follows:

1. For the outer region of the disk, $\sigma_t > \sigma_r > 0$ for $x_c \leq x \leq 1$.

(*a*) Equation 11*a* is used to determine σ_{t_c}/σ_a for given values of l, m, x_c, σ_o/σ_a and σ_{r_o}/σ_a (as shown in Figs. 3 and 4). The value of σ_o is obtained from tension creep test data of the disk material at elevated temperatures, and σ_{r_o} is obtained from the total calculated centrifugal force of the turbine blades transmitted through the rim of the disk to the disk proper.

(*b*) The value of σ_{t_c}/σ_a as determined in step (*a*) is next substituted into Eq. 12 and the critical value of x_c is found and checked against the assumed value of x_c in Eq. 11*a* (as shown in Figs. 3 and 4 or similar charts).

(*i*) If the value of x_c found by Eq. 12 is smaller than or equal to that assumed in Eq. 11*a*, then the condition $\sigma_t > \sigma_r > 0$ for $x_c \leq x \leq 1$

is satisfied and this value of σ_{t_c}/σ_a and the assumed value of x_c in Eq. 11a can be used for further calculations or follows.

(*ii*) If the value of x_c found by Eq. 12 is greater than that assumed in Eq. 11a, then the above condition will be not satisfied and steps (*a*) and (*b*) must be repeated, assuming a larger value of x_c in Eq. 11a, until the value of x_c found by Eq. 12 is smaller than or equal to that assumed in Eq. 11a. In this particular case, it would be convenient to have Figs. 3 and 4 or similar charts for guidance, to determine σ_{t_c}/σ_a and the corresponding assumed value of x_c.

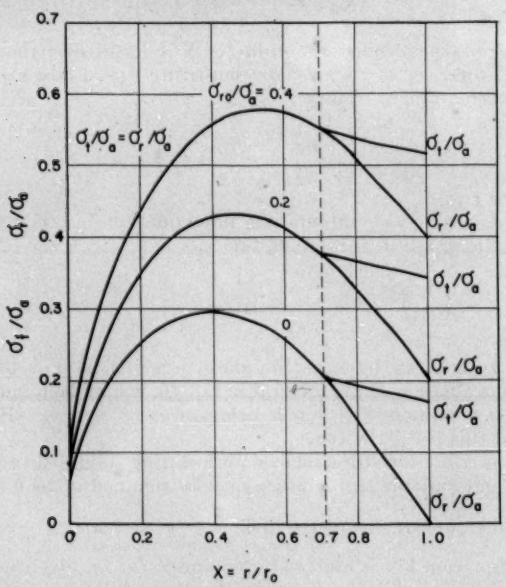

FIG. 7. Creep stresses in rotating solid disk, $l = 2.5$, $m = -0.5$, $x_c = 0.7$.

(*c*) Introducing these values of x_c and σ_{t_c}/σ_a from (*b*) to Eqs. 9a and 10a, the stress distribution of σ_t/σ_a and σ_r/σ_a are then determined and the condition $\sigma_t > \sigma_r > 0$ for $x_c \leq x \leq 1$ is satisfied.

2. For the inner region of the disk, $\sigma_t = \sigma_r > 0$ for $x_i \leq x \leq x_c$ and $\frac{1}{2} \leq \lambda \leq 1$.

(*a*) Equation 13a is used to compute $\sigma_t/\sigma_a = \sigma_r/\sigma_a$ after the values of σ_{t_c}/σ_a and x_c are substituted from step 1*b* above.

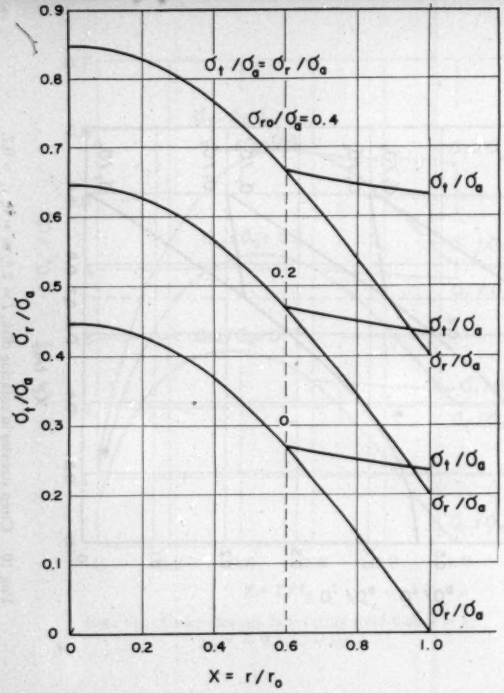

FIG. 8. Creep stresses in rotating solid disk, $l = 1.5$, $m = 0$, $x_c = 0.6$.

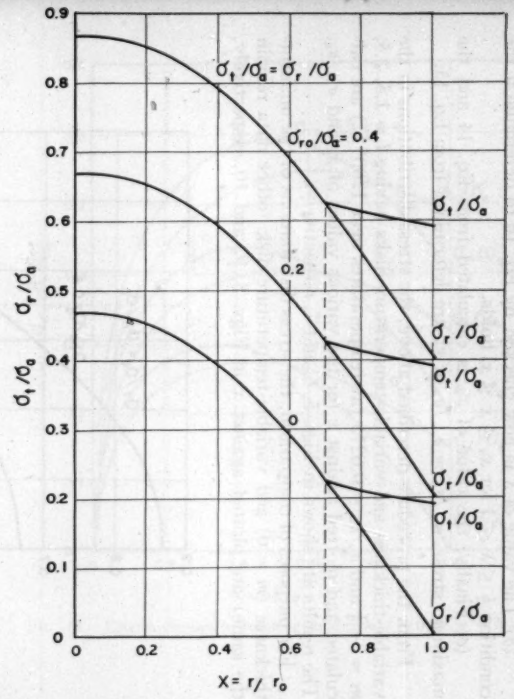

FIG. 9. Creep stresses in rotating solid disk, $l = 1.5$, $m = 0$, $x_c = 0.7$.

(*b*) The value of λ is now checked by Eq. 16 to determine if the condition $\frac{1}{2} \leq \lambda \leq 1$ for $x_i \leq x \leq x_e$ holds.

(*c*) Finally, the value of x_m is calculated from Eq. 14 and the maximum stress, $\sigma_{tm}/\sigma_a = \sigma_{rm}/\sigma_a$ at x_m are determined from Eq. 15.

From the procedure described above, the stress distributions in the variable-thickness and variable-temperature disks having $l = 1.5, 2.5$, $m = -\frac{1}{2}$ and $\sigma_e/\sigma_a = 0.0275$ (at temperatures near 1200° F.) are calculated and plotted against x for the various values of x_e and σ_{re}/σ_a. The results are shown in Figs. 5, 6, and 7, respectively.

For purposes of comparison, the stress distributions of the uniform-thickness ($m = 0$) and variable-temperature disk (other data remain the same) are plotted against x in Figs. 8, 9, and 10, respectively.

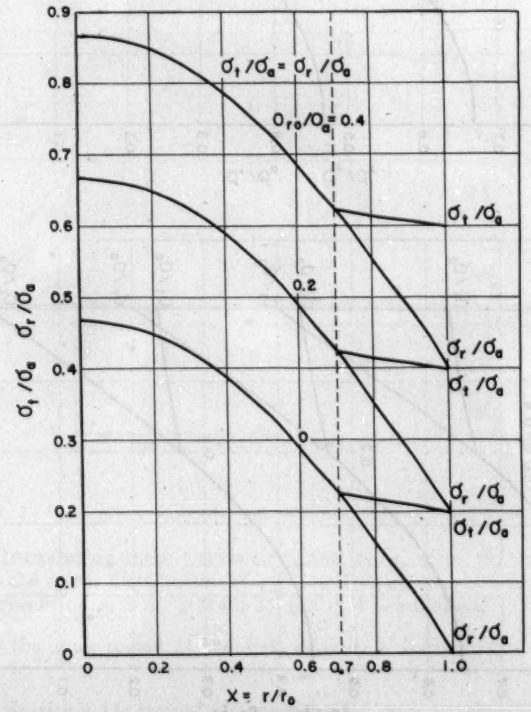

FIG. 10. Creep stresses in rotating disk, $l = 2.5$, $m = 0$, $x_e = 0.7$.

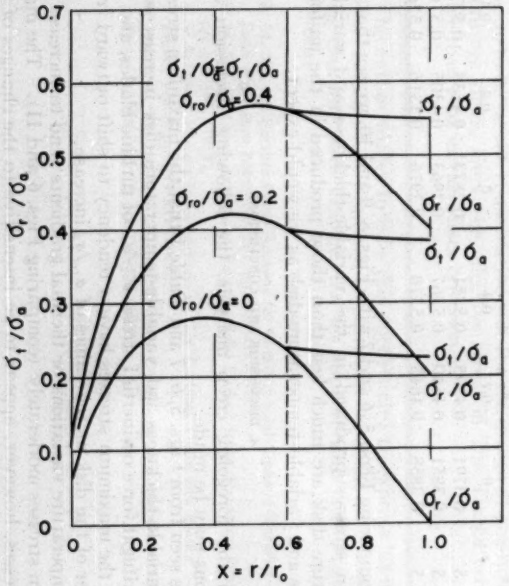

FIG. 11. Creep stresses in rotating solid disk, $l = 0$, $m = -0.5$, $x_a = 0.6$.

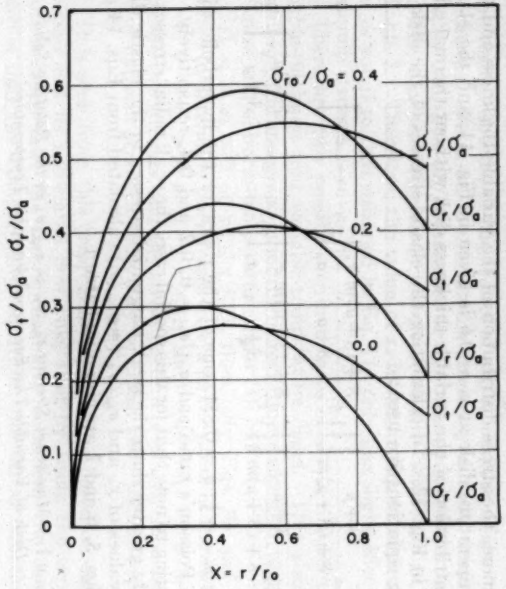

FIG. 12. Elastic stresses in rotating solid disk, $l = 0$, $m = -0.5$.

Furthermore, the stress distribution of the variable-thickness and uniform temperature disk at $x_c = 0.6$ is given in Fig. 11, and the elastic stress distribution of the variable-thickness disk without thermal effect is given in Fig. 12. In calculating the elastic stresses of the disk the following equations are used:

$$\frac{\sigma_r}{\sigma_a}=\frac{3+\mu}{8+(3+\mu)m}\left[\left\{1+\frac{8+(3+\mu)m}{3+\mu}\frac{\sigma_{r_o}}{\sigma_a}\right\}x^{q_1-(1+m)}-x^2\right] \tag{17}$$

$$\frac{\sigma_t}{\sigma_a}=\frac{3+\mu}{8+(3+\mu)m}\left[\left\{1+\frac{8+(3+\mu)m}{3+\mu}\frac{\sigma_{r_o}}{\sigma_a}\right\}q_1x^{q_1-(1+m)}-\frac{1+3\mu}{3+\mu}x^2\right] \tag{18}$$

in which $m=-\frac{1}{2}$; $q_1=0.851$, one of the roots for the hyperbolic disk; $\mu = 0.3$, Poisson's ratio and $\sigma_{r_o}/\sigma_a = 0$, 0.2 and 0.4, respectively. It is interesting to note that for this special case, the peak radial stresses are invariably greater than the peak tangential stresses in the elastic disk.

The values of x_m and σ_{t_m}/σ_a ($=\sigma_{r_m}/\sigma_a$) calculated from Eqs. 14 and 15 for Figs. 5, 6 and 7 are given in Table I.

TABLE I.—*Maximum Stresses* $\sigma_{t_m}/\sigma_a = \sigma_{r_m}/\sigma_a$ *in the Rotating Solid Disk of Variable Thickness and Variable Temperature.*

$m = -0.5$

x_c	l	x_m			$\sigma_{t_m}/\sigma_a = \sigma_{r_m}/\sigma_a$		
	σ_{r_o}/σ_a	0	0.2	0.4	0	0.2	0.4
0.6	1.5	0.3791	0.4595	0.5351	0.2873	0.4238	0.5726
0.7	1.5	0.3851	0.4640	0.5367	0.2963	0.4305	0.5761
0.7	2.5	0.3858	0.4645	0.5370	0.2976	0.4316	0.5769

By comparing Figs. 5, 6 and 7 with Figs. 8, 9 and 10, we see that the maximum stresses produced in the variable-thickness and variable-temperature disk are much less than those produced in the uniform-thickness and variable-temperature disk as we would expect.

4. DISCUSSION AND CONCLUSIONS

From the foregoing creep analysis, the following discussion and conclusions may be made.

1. It is seen from Figs. 5, 6, 7 and Table I that the maximum stresses in the variable-thickness and variable-temperature disk increase with the centrifugal force or inertial stress, σ_{r_o}/σ_a, of turbine blades, and the peaks of the maximum stresses have a tendency to shift outward from the center of the disk as the values of σ_{r_o}/σ_a increase.

2. Temperature variations or thermal gradients tend to increase the maximum stresses moderately (comparing Figs. 6 and 11). The maximum stresses, however, appear to be insensitive to the changes of the temperature variation (from $l = 1.5$ to $l = 2.5$ in this particular case)

as the turbine speeds, or the values of σ_{r_o}/σ_a increase (Figs. 6 and 7). The thermal effects on the maximum stresses gradually diminish and probably vanish as σ_{r_o}/σ_a increases to the burst speed of the disks.

3. The maximum stresses increase very slightly with x_c, Figs. 5 and 6 or Table I. Therefore, the value of x_c found in Eq. 12 either smaller than or equal to that assumed in Eq. 11*a* only has slight effect on the maximum stresses.

4. There are two possible extreme cases of stress distributions for variable-thickness and variable-temperature disks. This also applies to uniform-thickness and uniform-temperature disks and to variable-thickness and uniform-temperature disks (1). If

(*a*) $\sigma_t > \sigma_r > 0$ at $x_i \leq x \leq 1$, then only Eqs. 9*a* and 10*a* are required to determine the stresses except at the point of the disk center.

(*b*) $\sigma_t = \sigma_r > 0$ at $x_i \leq x \leq 1$, then only Eq. 13 is needed to calculate the stresses, and the stress pattern is exactly like that in the disk of uniform strength (this may be called the "pseudo-exponential disk").

5. It is seen from this creep analysis which is based on the Tresca criterian and its associated flow rule, that by using the exponential function creep law, the incompressibility equation, the equilibrium equation and the compatibility equation; the stress equations were derived with simplicity and ease. In addition, this stress analysis appears to be on the conservative side for the design of gas-turbine and jet-entinge disks, since the effective stress in the Tresca criterion is higher than that in the Mises criterion.

Acknowledgment

The author wishes to take this opportunity to express his appreciation to Professor J. F. Stanfort, Department of Mechanical Engineering, South Dakota State College, for his support and encouragement of this work.

REFERENCES

(1) B. M. MA, "A Further Creep Analysis for Rotating Solid Disks of Variable Thickness," JOUR. FRANKLIN INST., Vol. 269, pp. 408–419 (1960).

(2) B. M. MA, "A Creep Analysis of Rotating Solid Disks," JOUR. FRANKLIN INST., Vol. 267, pp. 149–165, (1959).

(3) S. S. MANSON, "Stress Investigations in Gas Turbines Disks and Blades," *SAE Quart. Trans.*, Vol. 3, pp. 229–239 (1949).

(4) W. PRAGER, "On the Use of Singular Yield Conditions and Associated Flow Rules," *Trans. ASME*, Vol. 75, pp. 317–320 (1953).

A TECHNIQUE FOR STUDYING SUPERSONIC COMBUSTION

A technique for securing information on the combustion process at supersonic speeds has been developed by the National Bureau of Standards with the support of the Navy Bureau of Weapons and the Air Force Office of Scientific Research. The technique involves firing a missile at hypersonic velocities through a combustible gas. High-speed schlieren photography is used to obtain data concerning shape and detachment distance of the shock wave, gas density, and other effects. These data are evaluated to derive information on the combustion process in the vicinity of the missile.

This experimental method, devised by F. W. Ruegg of the combustion controls group, permits precisely controlled variation of such parameters as pressure, temperature, fuel, and speed over a wide range under realistic conditions and at very little cost. It can be employed to examine in advance some of the problems of stabilizing detonation waves on a stationary object in a moving combustible mixture. If the wave can be established at the front of the missile, the drag will be substantially reduced. Results of studies using this method might be applied to the generation of thrust by burning at supersonic velocities either on the exterior of a missile or within it. Also, the method should contribute to the design of flame holders for supersonic combustion.

During the investigation, laminar combustion in a supersonic stream was observed for what is believed to be the first time. An unusual occurrence was that of large-amplitude oscillations in the megacycle frequency range produced by the combustion process at the front of the missile.

The study of the combustion process in standing detonation waves and in supersonic streams is of great practical importance in the field propulsion of hypersonic missiles and planes. Extensive information obtained in tube experiments is available concerning moving, plane detonation waves, but this body of data cannot with any assurance be simply transposed to the converse situation of a moving gas and a stationary oblique wave on a solid object. Furthermore, the object itself may exert unforeseen influence.

Some information has recently been obtained on the action of both normal and oblique shocks in inducing combustion in closed ducts and in free jets. The results are somewhat ambiguous, however, because of fuel and air mixing problems that exist in streams at high speed and temperature. Also, the range of experimental conditions was limited

by difficulties encountered in attempting to produce high-speed streams at high stagnation temperature and pressure.

The technique developed at the Bureau overcomes these obstacles by creating conditions such that a shock wave is established ahead of a high-speed missile, and then determining the conditions required to induce combustion and observing the effects of the missile on the combustion process. The stagnation temperatures attained are realistic, and the results are not affected by the method of mixing air and fuel or by turbulence. The experiment can easily be modified to determine the effects of the temperature and pressure history of the combustible gas on the combustion in the shock wave.

The Bureau's experiments were performed at Mach numbers from 4.2 to 6.5 in a mixture of hydrogen (30 per cent by volume) in air. Combustion was initiated by means of compression and heating within the shock wave standing on the missile. Characteristics of the combustion process depended strongly on the Mach number and on the state of the gas ahead of the wave.

The experimental apparatus comprises three essential parts: a gun and a range that contains the missile and the test gas, an electronic time-delay-ratio generator that computes the time to fire a high-voltage flash lamp, and an optical system for schlieren photography.

In the experiments performed up to the present, 0.785-inch-diameter nylon spheres were used as missiles. The sphere is mounted in a 20-millimeter case containing a fast-burning gun powder and fired from a .60-caliber, 6-ft.-long test barrel through a blast chamber and the test section to a heavy metal target and trap. Two phototubes are located upstream of the test gas, which is isolated from the remainder of the system by two plastic diaphragms.

Elapsed time of flight of the missile between the two phototubes is measured by an electronic timer that counts the number of pulses from an oscillator operating at a frequency of one megacycle. Signals from the phototubes enter the time-delay-ratio generator, which computes the time of arrival of the missile at the photographic station and triggers the high-voltage flash lamp at that time. A second electronic timer measures the time between the missile's arrival at the second phototube and the time at which the lamp is flashed. Two speed measurements are thus available for calculating the deceleration of the missile in the test section.

HIGH-RESOLUTION CAMERA

A research camera capable of projecting a parallel line pattern of 50,000 lines per inch has been developed at the National Bureau of Standards. The camera, designed by C. S. McCamy of the Bureau's photographic research laboratory, is a step toward the development of a standard method for determining the resolving power of photographic materials.

At the present time, there is no standard method for measuring resolution. The Bureau's work is part of efforts by a committee of the American Standards Association to establish such a standard. Five laboratories in the United States and Canada are working on methods which can be employed. By comparison of results, they will be able to determine the factors which must be specified in order that all resolution tests on the same film or plate may yield the same result.

To insure that any limitations revealed by the test are those of the photographic materials and not of the test equipment, the camera must be able to produce a line pattern much finer than can be resolved by the emulsion being tested. To test the new camera's full capabilities (50,000 lines per inch) it was necessary to use extremely high-resolution spectrographic plates having a film speed of 0.025 when rated on the ASA scale for pictorial negative materials.

The camera's optical system is essentially a fine apochromatic microscope operated in reverse to make an extremely small image of a large chart. The camera has interchangeable lenses. Objectives in use are an 8-mm. lens having a numerical aperture of 0.65, which is equivalent to an *f*-number of 0.77, and a 16-mm. lens having a numerical aperture of 0.30 or an *f*-number of 1.66. For this application the elements of the objectives were respaced and the interiors of the lens mounts were specially blackened to minimize reflections.

Film or plates to be tested are placed against a surface attached to the objective lens mount by a fine screw thread, with a gear mechanism permitting minute adjustment of focus. Films are held in place by a miniature vacuum back. The focus is first set by direct visual observation with a microscope. Several exposures are then made, setting a slightly different focus each time, until the position of best focus is found. The camera is operated at a constant temperature to avoid changes in focus resulting from thermal expansion or contraction.

To secure even illumination of the targets to be photographed, a compensator plate is placed between the lamp and condensers of the camera's illuminating system. The compensator is a glass sheet with a circular pattern printed on it—heavier at the center than at the edges—which counteracts the tendency of the condensers to give higher illumination at the center of the beam. Provision has been made to place filters, either color temperature-correcting filters or neutral density filters, between the illumination and the test chart. Color correcting filters are used to adjust the illumination for the particular emulsion being tested. Neutral density filters are used to obtain a series of exposures of varying illuminance. The maximum resolving power obtained in the series is reported.

One important consideration in photographing the fine line patterns is to eliminate mechanical vibrations which could blur the photographs. To this end, the camera, including test chart, illuminator, shutter, and

optics is encased in a massive steel cylinder. The cylinder, in turn, is suspended from the ceiling by springs. The vibrations naturally present in the building were determined to be mainly 30 cps, 60 cps, and 120 cps; since the springs used for support have a natural frequency of approximately 2 cps, an effective mechanical insulation is achieved.

The new camera was used in an experiment to test the generally accepted correlation between resolving power and legibility at an extreme reduction ratio. In addition, the photograph made shows the extremely fine detail which may be recorded by this system.

In this experiment, Bernard Fouquet of the Bureau's photographic research laboratory made a photocopy of the first page of the Bible at a linear reduction ratio of 1000, thus reducing the *area* by a total factor of one million.

The page was first reduced 2.5 times to fit into the camera's chart holder; then it was reduced by a factor of 400 with the new camera. If the entire Bible could be reproduced at this reduction ratio, it would cover no more than $\frac{1}{4}$ cm^2, less than the area of Lincoln's head on a penny.

The microcopy was made on a high-resolution spectrographic plate using an exposure of 10 sec at $f/0.77$. It is clearly legible when viewed directly at a magnification of 1250× through a fine optical microscope. Blue light is used to view the microcopy since a short wavelength enhances resolution.

The Bureau does not recommend this method for routine microcopying. Because of the difficulty in focusing, the problem of keeping dust from the field, the long exposures involved, and the difficulty of viewing the copy, the method is too tedious for routine use.

Since one of the main purposes of the undertaking was to develop a standard method of measuring resolving power of photographic materials, the materials and components used were deliberately limited to those generally available. Somewhat better performance might be realized if this limitation were relaxed. Much more work remains to be done before a method can be standardized.

BOOK REVIEWS

STATISTICAL THEORY OF COMMUNICATION, by Y. W. Lee. 509 pages, diagrams, 6 × 9 in. New York, John Wiley & Sons, Inc., 1960. Price, $16.75.

This book, written primarily for the first-year graduate student in electrical engineering, presents clearly and rigorously a physically motivated and systematic account of the statistical theory of communication. The author has pioneered in the synthesis of electric networks by means of the Fourier transforms of Laguerre's functions and is co-inventor (with Dr. Norbert Wiener) of such networks in the time domain and the frequency domain. Dr. Lee and Dr. Wiener set forth for the first time in the history of circuit theory the amplitude-phase relations in system functions, and the real part and imaginary part relations in these functions, in the form of Hilbert transforms. So, when the author says in his Preface that he does not attempt to cover the subject of study but attempts to uncover it for the student, there comes a stimulating book on the fundamental theory of communication.

The reviewer was aware of the intimate cooperation between Wiener and Lee when he was able to invite Dr. Wiener to visit Tsing Hua University for the academic year 1935–36 so that they could work together. In his book "*I Am a Mathematician*" (Doubleday and Company, Inc., Garden City, N. Y., 1956), Wiener said: "If I were to take my specific boundary point in my career as a journeyman in science and as in some degree an independent master of the craft, I should pick out 1935, the year of my China trip, as that point." After World War II, Dr. Lee was invited to teach at M.I.T., and he has stayed on teaching and doing research since 1946. Quoting Wiener again: "What made Lee's situation easier was that I had recently developed a considerable part of the statistical theory of communication engineering . . . . Thus, he took over the problem of working out in detail the communication and engineering consequences of ideas which I had only sketched in general terms and of making himself interpreter to the engineering public of the field which I was later to call cybernetics."

The book starts with a short introduction which refers to the classic work of Wiener entitled "The Extrapolation, Interpolation, and Smoothing of Stationary Time Series with Engineering Applications" (John Wiley & Sons, New York, 1949). Chapters 2 to 8 give the basic concepts and tools which are summarized in Chapter 9. These chapters cover generalized harmonic analysis, probability, random variables, ensembles, and distributions, time averages and ensemble averages, correlation functions and power density spectrums of random processes. In Chapter 9, the author said:

> Messages and noise are not completely predictable so that unique specification of these functions for all values of time is contrary to their nature . . . . A meaningful and useful method of description has been found to be the description by a set of probability densities (probability distributions if the ensemble is discrete). This is a fundamentally different concept in describing functions as compared with the concept of complete determinism and the concept of amplitude and phase spectrums for periodic and aperiodic functions.

The next eight chapters cover such important topics as sampling theory, detection of a periodic signal in noise, optimum linear systems, optimum filtering and prediction, errors in optimum systems, and theory of optimum systems. The fundamental relations for a linear system discussed in Chapter 13 include the input-output relation in autocorrelation, the input-output crosscorrelation theorem, and the crosscorrelation of linearly transformed random functions. In Chapter 17 optimum systems are studied both on the minimum-integral-square-crosscorrelation-error criterion and with transient inputs on the minimum-integral-square-error criterion.

The last two chapters—Chapters 18 and 19—deal with the application of orthonormal functions to the representation of correlation

functions and power density spectrums and to the synthesis of optimum linear systems. As the author said in the Preface:

> . . . However, because of the great importance of the orthonormal representation of a linear system in the statistical theory of optimum nonlinear systems, as discussed by Professor Wiener in his book *Nonlinear Problems in Random Theory*, the last chapter of the book is devoted to the synthesis of linear systems by orthonormal functions.

When the reviewer was Visiting Professor at M.I.T. in 1950–52, Professor Lee was already well established in this new field and had started to write this book. It has taken him a rather long time to finish the manuscript as he wanted to present the material as clearly and rigorously as possible. It is the reviewer's great privilege to recommend this carefully written treatise on the modern statistical theory of communication to the engineering public. The author has ably demonstrated the importance of this new field which is "a landmark in the history of communication theory."

Y. H. KU
University of Pennsylvania

JET PROPULSION ENGINES, edited by O. E. Lancaster. 799 pages, plates 6 × 9¼ in. Princeton, Princeton University Press, 1959. Price, $20.00.

This book consists of a group of well integrated articles on jet propulsion. Beginning with its historical development, chapters on general formulas, cycle analysis, matching components, engine performance, with interesting chapters on fuels, ram rockets, helicopter jet rotors and atomic energy applications cover a wide range of technical information on this subject.

The entrance chapter by F. J. Malina gives an interesting discussion of the history of developments, including R. H. Goddard's pioneer experiments. It is impressive to note his introduction of the converging-diverging nozzle for increasing jet speeds above the acoustic velocity, enormously upping the efficiency, with ejection velocities increased from 1000 to over 8000 ft/sec.

Chapter I by Maurice Roy covers a detail analysis on the interaction of flows with the engine and airplane exterior. The effective thrust is divided correctly into interior and external components. Next the momentum change of the flow through engine is determined, where the housing reaction and end pressures at exit and entrance are considered. The latter are determined by an analysis of entrance and exit flow conditions. These are complicated by the interaction of internal and external flow which takes place at the ends, as well as the appraising of the latter, and its drag reaction on the exterior of the engine housing.

In a succeeding Chapter C, C. A. Meyer follows a similar approach, along with discussions of experimental data on axial and centrifugal compressors, burners, and performance matching. The experimental data and discussions are worthy of study. Section D by Driggs and Lancaster covers very useful studies relating to performance analysis, propeller performance, turbine design, controls, gear box and accessories, as well as engine testing methods.

The general discussion on ram jets by DeMarquis, D. Wyatt and Bruce T. Lundin is extensive and most interesting. Similar studies are not likely to be found elsewhere. Special chapters on intermittent jets by Joseph V. Foa include propulsive cycles, the pulse jet and wave engines.

Section G by Martin Summerfield on the liquid propellant rocket engine is a valuable discussion of basic thermodynamic relations as to the nature of combustion and nozzle performance with liquid fuels. It includes cooling problems of rocket motors.

Section H, by C. E. Bartley and Mark M. Mills covers the interior ballistics of solid propellants. This important subject is well treated and gives features on mechanical design as well.

The Ram Rocket, by Irvin Glassman and Joseph V. Charyk, is of special interest in its relation with the ram jet, as well as the general problem of mixing and combustion of two or more dissimilar streams. The work covers considerable analysis as well as experimental performance evaluation.

The chapters by Albert Gail on Jet Rotors cover the kinematics and blade propulsion reactions with jet motors. This extends to helicopter jet rotor performance, including mechanical design.

A final chapter on the application of atomic energy in jet propulsion is covered in a com-

prehensive way by Ralph Zirkind. Reactor design, shielding and general systems of heat transfer through liquid metals to turbo jet radiators are accompanied by preliminary design data.

A closing chapter by F. Zwicky discusses the future prospects of jet propulsion.

In spite of the outstanding array of very worthwhile technical discussions, covering a fair range of the subject, it would seem an over-all basic analysis on the reaction of fluids, particularly as to the nature of energy transfer and thermodynamic relations between the flow and engine housing and jet, and the significance of propulsion efficiency, should be included in a condensed entrance chapter.

On the whole, this book should prove of great value to all technical engineers concerned with jet propulsion.

RUPEN EKSERGIAN
The Franklin Institute Laboratories

REACTOR ANALYSIS, by Robert V. Meghreblian and David K. Holmes. 808 pages, illustrations, 6 × 9 in. New York, McGraw-Hill Book Co., Inc., 1960. Price, $19.50.

This volume is by far the most complete and extensive treatise on the analytical methods used in the study of the properties and behavior of nuclear fission reactors. The content of the book is an extension of the notes developed by the authors for a course given by them for several years at the Oak Ridge School of Reactor Technology (ORSORT) at the Atomic Energy Commission's Oak Ridge National Laboratory.

The subject of reactor analysis deals with the methods and mathematical models used in predicting the spatial, temporal and energy distributions of the neutron population in assemblies containing fissionable substances. Since the authors emphasize the methods of analysis rather than the physical processes themselves, this test serves to complement another recent book which places its major emphasis on the physical aspects of fission reactors ("The Physical Theory of Neutron Chain Reactors," by A. M. Weinberg and E. P. Wigner). It should be noted that both these books cover much the same subjects, and both present the descriptions of the physical phenomena, the theories, and the formulations of methods of analysis; it is in their placing of emphasis in which they differ.

The authors have proceeded logically through the principal topics of reactor analysis. Beginning with an introductory discussion which describes the various types of nuclear reactors and the various problems confronting the reactor physicist (Chapter 1), they proceed through extensive presentations of probability concepts (including nuclear cross sections) and neutron multiplication and flux (Chapters 2 and 3, respectively). There then follows a group of chapters with each devoted to a separate major topic: slowing-down in an infinite medium, diffusion theory, Fermi age theory, transport theory, reflected reactors, reactor kinetics, and heterogeneous reactors. The book concludes with three chapters covering relatively advanced subjects: control-rods, hydrogenous systems, and perturbation theory.

The discussion of each method or model is presented in considerable detail in order to emphasize the approximation and limitations attendant to each. The authors have attempted to present the most suitable applications for each of the theoretical models discussed, and have in a majority of instances demonstrated the general procedure by means of a numerical example. The subjects discussed are well documented by means of footnotes. A group of problems associated with the various topics is also included following many of the chapters.

The authors have intended this text for the graduate engineering student. Although it is well suited as both an introductory and an advanced text on reactor analysis, a basic nuclear physics background is presupposed, and the student or reader acquainted with the various types of reactor physics problems will better appreciate the utility of the different analytical models and the circumstances under which each is most useful. The authors have succeeded in writing an exceptionally clearly written text which presents the theories and the basic methods available for determining neutron-density distributions in various reactor configurations. The book is best suited for those intending to specialize in reactor physics or reactor analysis, although anyone who has the proper background in engineering mathematics could profit from its study.

W. H. STEIGELMAN
The Franklin Institute Laboratories

BOOK NOTES

THE MAJOR ACHIEVEMENTS OF SCIENCE, by A. E. E. McKenzie. Vol. I, 368 pages, plates, diagrams, 5½ × 8½ in. Price, $5.50. Vol. II, 195 pages, illustrations, 5½ × 8½ in. Price, $3.50. New York, Cambridge University Press, 1960.

This two-volume work covers the history of the main developments in science from ancient times to the present. In the 24 chapters comprising Vol. I, the author describes such general concepts as the Copernican theory, the circulation of the blood, the creation of modern chemistry, the atomic theory, the wave theory of light, evolution, the clash between science and religion, the theory of relativity, the quantum theory and the latest theories about the creation of the universe. In addition to relating events leading up to the specific development, Mr. McKenzie gives background information on the discoverer of the development and describes the effect of the discovery on contemporary society. The author has skillfully blended his capsule views of the important discoveries and developments in science into an over-all picture of their influence on Western thought and civilization. In Vol. II, Mr. McKenzie has collected 91 extracts from original writings of the scientists whose theories he expounded in Vol. I. Arranged under the same chapter headings as Vol. I, these original writings have been carefully chosen from books, lectures and letters rather than the highly scientific papers of the men, so that the general reader may obtain an insight into the personalities of the men responsible for our scientific advances.

INFRARED METHODS: PRINCIPLES AND APPLICATIONS, by G. K. T. Conn and D. G. Avery. 203 pages, diagrams, 6 × 9 in. New York, Academic Press, 1960. Price, $6.80.

The authors have prepared this introduction to infrared studies primarily for the research student in physics, chemistry, boichemistry, biology and medicine, because " . . . we believe that there is no other working manual." Dividing the book into two parts, the authors cover principles in Section A and practical applications in Section B. Part A includes sources of radiation, optical materials, detectors, amplifiers and dispersive systems. Part B is devoted to calibration of detectors, simple monochromators, instruments for gas analysis, and radiation pyrometry. The book is restricted to the "near infrared"—the range from 1 to 25 μ. One of its best features is the inclusion of over 500 references, divided among the chapters and covering the period from 1863 through 1959.

QUALITATIVE THEORY OF DIFFERENTIAL EQUATIONS, by V. V. Nemytskii and V. V. Stepanov. 523 pages, 6 × 9 in. Princeton, Princeton University Press, 1960. Price, $12.50.

This translation, based on the enlarged and revised second Russian edition, is No. 22 of the Princeton Mathematical Series. Part One (306 pages), dealing with classical differential equations, has four chapters: Existence and Continuity Theorems; Integral Curves of a System of Two Differential Equations; Systems of n Differential Equations; and A Study of Neighborhoods of Singular Points and of Periodic Solutions of Systems of n Differential Equations. In addition, there is a translation of a resume written by Nemickii of work done on qualitative theory (not included in the Russian work). Part Two (217 pages) covers topological dynamics and ergodic theory.

MODERN NUCLEAR TECHNOLOGY, edited by Mark M. Mills, Arthur T. Biehl and Robert Mainhardt. 336 pages, illustrations, 6 × 9 in. New York, McGraw-Hill Book Co., Inc., 1960. Price, $9.50.

This book is comprised of a series of lectures given under the Engineering Extension Program of the University of California during the summers of 1956 and 1957. Approxi-

mately twenty-two guest speakers, all specialists in the field, participated in the course entitled, "A Survey of Nucelar Engineering for Management." The purpose of this survey course was to present on a management level the fundamentals of nuclear engineering, in order to help management personnel understand some of its problems. Basic engineering principles or method of approach for the solution of engineering problems are therefore not discussed. The presentation of material is then directed toward the mature industrialist with an engineering degree, but inactively engaged in engineering for five to ten years.

ELECTRICAL NOISE, by W. R. Bennett. 280 pages, diagrams, 6 × 9 in. New York, McGraw-Hill Book Co., Inc., 1960. Price, $10.00.

This book presents a comprehensive account of how noise originates in electrical circuits, how it is measured, and how circuits may be designed to minimize undesirable effects from noise. It describes in qualitative terms the physical nature of various important noise sources, including thermal agitation or resistance noise, shot noise in vacuum tubes and semi-conductor junctions, noise from spontaneous emission of electromagnetic radiation, and noise in gas discharges. The fundamentals needed for analyzing basic sources of noise are stressed as well as the methods of measurement and design. In addition to the standard theory of noise figure and its significance, a treatment of the more comprehensive Haus-Adler theory of noise measure is given. The author also reviews noise in the various methods of signal transmission such as amplitude modulation, frequency modulation, and the different kinds of pulse modulation.

MANAGEMENT CONTROL SYSTEMS, edited by Donald G. Malcolm and Alan J. Rowe. 375 pages, diagrams, 6 × 9 in. New York, John Wiley & Sons, Inc., 1960. Price, $7.25.

These are the proceedings of a symposium held at the System Development Corporation in Santa Monica, California, July 29–31, 1959. A comprehensive treatment on management controls by some thirty experienced individuals in all areas of management is presented in this volume. The editors and contributors have constructed a case for "designed" controls to produce better results in management patterns now and for the long-range future. The problem of designing adequate controls is herein given careful consideration, especially in relation to the fact that the design of systems is currently at best a systematic process rather than one where analytical evaluation is possible. Special attention is given to computers and their role in this problem. Contributors to this symposium have described and weighed the advantages of using computer applications to simulate company activities so as to create a management-laboratory where the effects of policy and procedures can be tested and evaluated prior to their adoption.

COMPUTER LOGIC: THE FUNCTIONAL DESIGN OF DIGITAL COMPUTERS, by Ivan Flores. 458 pages, diagrams, 6 × 9 in. Englewood Cliffs, New Jersey, Prentice-Hall, Inc., 1960. Price: $12.00 (trade); $9.00 (text).

This volume is the first of its kind to offer a complete block diagram analysis of each operational unit of a digital computer—describing and illustrating in detail just how a computer is put together and how it works. The author emphasizes the organization and functional interrelation of fundamental units and discusses these relationships from the viewpoint of operational necessity rather than mathematical logic, Boolean algebra or circuit theory. Especially helpful to the reader is the extensive treatment given two often-neglected topics: (1) input/output and (2) control of computer function. Problems are included that provide a means of acquiring facility with computer terms, and the final chapter reviews in detail what happens from the time the programmer receives the problem until the answer is ready. A complete glossary of terms is provided at the end of the book.

ELECTRICAL ENGINEERING PROBLEMS, by E. M. Williams and F. J. Young. 294 pages, diagrams, 6 × 9 in. New York, McGraw-Hill Book Co., Inc., 1960. Price, $7.75.

A collection of engineering problems ideally suited for laboratory activities is presented in this volume. Ranging from intermediate

to advanced the problems include such subjects as linear and nonlinear d-c and a-c circuits, electromechanical devices, transformers, magnetic-core switching circuits, rotating-machines, and vacuum and semiconductor electronic circuits. The problems have all been laboratory tested during the past decade in various courses at Carnegie Institute of Technology which stress laboratory problem-solving disciplines. The book is particularly suitable for electrical engineering work, but can be used in the laboratory of a variety of courses, such as circuits, electronics, and mechanics.

PROCEEDINGS OF THE SECOND CONFERENCE ON REACTIONS BETWEEN COMPLEX NUCLEI, edited by A. Zucker, E. C. Halbert and F. T. Howard. 319 pages, illustrations, 8½ × 11 in. New York, John Wiley & Sons, Inc., 1960. Price, $7.00.

This book contains all forty research papers presented at this conference held in Gatlinburg, Tennessee, May 2–4, 1960, and includes transcripts of the discussions which followed them. The papers are grouped into five sections to correspond to topics of the five conference sessions—transfer reactions; Coulomb excitation; scattering; transuranium, fission and low energy Li reactions; and compound nucleus reactions. In addition there is a summary of the conference by Prof. E. P. Wigner. These theoretical and experimental papers by distinguished scientists from Canada, Great Britain, Switzerland, USSR, as well as the United States, represent the results of various research projects, interpretation of these results, and discussion of their relation to the present body of knowledge about atomic nuclei.

THYRATRONS, by C. M. Swenne. 73 pages, plates, diagrams, 5¾ × 8¼ in. New York, The Macmillan Company, 1960. Price, $3.00.

This book is written for the engineer who is already familiar with electrical engineering but who needs further study to keep up with industrial electronics. In four chapters the author covers physical principles, electrical characteristics, basic circuits, and applications of thyratrons (in relay circuits, electronic timers, controlled rectifiers, control circuits and inverters). The presentation is not cluttered up with mathematics; rather, it is a practical treatise, with descriptions and applications set forth in plain language. An N. V. Phillips' publication, it is published in English (Macmillan), French, German, Spanish and Dutch.

STATISTICAL THEORY AND METHODOLOGY IN SCIENCE AND ENGINEERING, by K. A. Brownlee. 570 pages, 6 × 9 in. New York, John Wiley & Sons, Inc., 1960. Price, $16.75.

In preparing this elementary text on statistical methods, the author has " . . . leaned towards attempting to convey understanding of principles rather than practice, a choice rationalized on the ground that at this mathematical level the market is better provided with textbooks for the latter than the former." The student is assumed to know exponents, logarithms, and simple algebraic manipulation. The main topics covered are discrete distribution, nonparametric tests, analysis of variance, and regression and correlation. The Appendix contains ten tables of useful data, including percentage points of the t, χ^2 and F distributions, random sampling numbers, etc.

PUBLICATIONS RECEIVED

FROM THEORY TO PRACTICE IN SOIL MECHANICS. Selections from the writings of Karl Terzaghi, with bibliography and contributions on his life and achievements prepared by L. Bjerrum, A. Casagrande, R. B. Peck and A. W. Skempton. 425 pages, illustrations, 8½ × 11 in. New York, John Wiley & Sons, Inc., 1960. Price, $12.00.

BOUNDARY LAYER THEORY, by Hermann Schlichting, translated by J. Kesten. Fourth edition, 647 pages, illustrations, 6¼ × 9¼ in. New York, McGraw-Hill Book Co., Inc., 1960. Price, $16.50.

HANDBOOK OF LAPLACE TRANSFORMATION: TABLES AND EXAMPLES, by Floyd E. Nixon. 115 pages, 5 × 8 in. Englewood Cliffs, Prentice-Hall, Inc., 1960. Price: $6.00 (trade); $4.50 (classroom).

PERIODICALS IN THE CHEMICAL SOCIETY LIBRARY. 48 pages, 6¼ × 8¼ in. London, The Chemical Society, 1960. Price, 5 shillings.

CLASSICS IN SOCIOLOGY. A course of selected reading by authorities, with an introductory reading guide by Donald MacRae. 326 pages, 5¾ × 9 in. New York, Philosophical Library, 1960. Price, $6.00.

CLASSICS IN WESTERN CIVILIZATION. A course of selected reading by authorities, with an introductory reading guide by D. C. Somervell. 338 pages, 5¾ × 9 in. New York, Philosophical Library, 1960. Price, $6.00.

CLASSICS IN BIOLOGY. A course of selected reading by authorities, with an introductory reading guide by S. Zuckerman. 351 pages, 5¾ × 9 in. New York, Philosophical Library, 1960. Price, $6.00.

CLASSICS IN SCIENCE. A course of selected reading by authorities, with an introductory reading guide by E. N. Da C. Andrade. 322 pages, 5¾ × 9 in. New York, Philosophical Library, 1960. Price, $6.00.

READABLE RELATIVITY, by Clement V. Durell. 146 pages, diagrams, 5¼ × 8 in. New York, Harper & Brothers, 1960. Harper Torchbook No. 530. Price, $1.25 (paper).

A HISTORY OF THE THEORIES OF AETHER & ELECTRICITY, by Sir Edmund Whittaker. New York, Harper & Brothers, 1960. Harper Torchbooks Nos. 531 and 532. Vol. I: The Classical Theories, 434 pages, 5¼ × 8 in. Price, $1.95 (paper). Vol. II: The Modern Theories, 319 pages, 5¼ × 8 in. Price, $1.85 (paper).

CONCEPTS OF SPACE, by Max Jammer, with foreword by Albert Einstein. Reprinted from the 1954 edition. 208 pages, 5½ × 8 in. New York, Harper & Brothers, 1960. Harper Torchbook No. 533. Price, $1.40 (paper).

THE FOUNDATIONS OF ARITHMETIC, by Gottlob Frege, translated by J. L. Austin. 119 pages, 5¼ × 8 in. New York, Harper & Brothers, 1960. Harper Torchbook No. 534. Price, $1.25 (paper).

LECTURES ON THEORETICAL RHEOLOGY, by M. Reiner. Third edition, 158 pages, illustrations, 5¾ × 8½ in. New York, Interscience Publishers, 1960. Price, $4.85.

THE FRANKLIN INSTITUTE

Minutes of the Stated Meeting

December 21, 1960

The Stated Meeting of The Franklin Institute was held at 8:15 P.M. in the Lecture Hall, preceded by a dinner in Franklin Hall at which Silver Members of 1960 were honored. Wynn Laurence LePage, President, called the meeting to order with approximately 120 members and guests present.

The President stated that the minutes of the Stated Meeting of October 19, 1960 were published in the November issue of the JOURNAL. There being no corrections, the minutes were approved as published. He stated the minutes of the Stated Meeting of November 16, 1960 will be published in the next issue of the JOURNAL and will be presented at the Annual Meeting in January 1961 for approval.

The President announced that at the Annual Meeting of The Institute to be held on January 18, 1961, ten members are to be elected to the Board of Managers for a term of three years beginning in 1961, and that the Secretary had informed him that eleven nominees had been named and nominations were closed fifteen days before the Stated Meeting in accordance with the By Laws. For the Chairman of the Nominating Committee, the Secretary read the following report:

"Under the provisions of Article VIII, Section 3 and Article IV, Section 5, of the By Laws, the following eleven names have been properly placed in nomination to fill the ten vacancies on the Board of Managers which will occur at the Annual Meeting of The Institute on January 19, 1961.

Morton Gibbons-Neff	1944*	Henry B. Bryans	1951	Emery W. Loomis	1954
Rupen Eksergian	1945	Wynn Laurence LePage	1953	Henry M. Chance, II	1958
Francis J. Chesterman	1949	Gaylord P. Harnwell	1954	Joseph A. Fisher	1959
James Creese	1950			Kenneth Robert Atkins	

"The Nominating Committee is required by the By Laws to submit to the membership at this meeting its recommendations with respect to the candidates.

"Accordingly, the Nominating Committee recommends to the membership that the following ten gentlemen be elected to fill the vacancies which will exist. All the recommended nominees are currently members of the Board of Managers:

Morton Gibbons-Neff	James Creese	Emery W. Loomis
Rupen Eksergian	Henry B. Bryans	Henry M. Chance, II
Francis J. Chesterman	Wynn Laurence LePage	Joseph A. Fisher
	Gaylord P. Harnwell	

"The ballot will include all the nominees and the recommendations of this Committee will be indicated."

The President appointed the following Tellers of Election, in accordance with the By Laws, who are neither officers nor nominees: Alfred W. Duerig, Dr. Joseph S. Hepburn, John H. Neher.

Mr. LePage spoke briefly of some of the things that are in prospect for The Franklin Institute. Taking seriously the announcement of the President of the United States some eighteen months ago that science education was a national policy, and giving serious thought to the part The Institute has played in science education during the past 136 years, the Managers requested a survey be made to appraise the work of the Institute in this field. This was made possible by a grant from the Dolfinger-McMahon Foundation. Using this survey, a long-range program for science education was developed. To give financial support to carry out this program, we have the assistance of leading citizens of the Philadelphia area, including one of our own members, John A. Diemand, President of The Insurance Company of North America, who has consented to be General Chairman of the Drive for funds for The Franklin Institute Development Program. But The Franklin Institute is more than a science museum and planetarium. Here we conduct research and development work for industry and the government. We have launched a program to procure long-needed facilities for The Franklin Institute Laboratories for Research and Development and we will enter into a long-term lease for a research center to be built in an area adjacent to The Franklin Institute's main building.

In presenting the speaker of the evening, Miss Beth Peterson, Home Economist for the Extension Division of the E. I. duPont de Nemours & Company, Mr. LePage commented that he believed Miss Peterson was the first lady speaker to grace our platform. Miss Peterson's talk on "Fibers, Facts and Fashions" was a fascinating description of the newer fibers and fabrics and the research required not only to manufacture the fabrics but to determine consumer requirements. Following the talk, members and guests were invited to inspect the samples of fabrics which were beautifully displayed in the front of the hall.

The President expressed warm thanks to Miss Peterson for her delightfully interesting talk, and adjourned the meeting at 9:50 P.M.

WILLIAM F. JACKSON, JR.
Secretary

* Year first elected to Board of Managers.

NEW BOOKS IN THE FRANKLIN INSTITUTE LIBRARY

MATHEMATICS

FUNDAMENTALS OF SIGNAL THEORY, by J. L. Stewart. McGraw-Hill, 1960.

OPERATIONS RESEARCH AND SYSTEMS ENGINEERING, by C. D. Flagel. Johns Hopkins Press, 1960.

SAMPLE DESIGN IN BUSINESS RESEARCH, by W. E. Deming. Wiley, 1960.

THE THEORY OF STORAGE, by P. A. P. Moran. Wiley, 1959.

ADVANCED ENGINEERING MATHEMATICS, by C. R. Wylie. 2nd ed. McGraw-Hill, 1960.

ELECTRONIC COMPUTERS, by T. E. Ivall. 2nd ed. Philosophical Library, 1960.

OPERATIONS RESEARCH, by J. H. Batchelor. 2nd ed. Saint Louis University Press, 1959.

INFORMATION AND DECISION PROCESSES, by R. E. Machol. McGraw-Hill, 1960.

DIGITAL COMPUTERS AND NUCLEAR REACTOR CALCULATIONS, by W. C. Sangren. Wiley, 1960.

CONTRIBUTIONS TO PROBABILITY AND STATISTICS; essays in honor of Harold Hotelling, edited by Ingram Olkin. Stanford University Press, 1960.

INTRODUCTION TO LAPLACE TRANSFORMS FOR RADIO AND ELECTRONIC ENGINEERS, by W. D. Day. Interscience, 1960.

STATIONARY PROCESSES AND PREDICTION THEORY, by H. Furstenberg. Princeton University Press, 1960.

INTRODUCTION TO LINEAR PROGRAMMING, by W. W. Garvin. McGraw-Hill, 1960.

RIEMANN SURFACES, by L. V. Ahlfors. Princeton University Press, 1960.

INTERNATIONAL CONFERENCE ON INFORMATION PROCESSING. Proceedings. UNESCO, 1959.

DESIGN FOR A BRAIN, by W. R. Ashby. 2nd ed. Wiley, 1960.

INTERNATIONAL CONFERENCE ON SCIENTIFIC INFORMATION. Proceedings. National Research Council, 1959.

AUTOMATIC LANGUAGE TRANSLATION, by A. G. Oettinger. Harvard University Press, 1960.

PHYSICS

THE SCATTERING AND DIFFRACTION OF WAVES, by R. W. King. Harvard University Press, 1959.

INTRODUCTION TO QUANTUM MECHANICS, by R. H. Dicke. Addison-Wesley, 1960.

REACTOR ANALYSIS, by R. V. Meghreblian. McGraw-Hill, 1960.

CONCEPTS OF THERMODYNAMICS, by E. F. Obert. McGraw-Hill, 1960.

NUCLEAR SPECTROSCOPY, edited by F. Ajzenberg-Selove. Academic Press, 1960.

WAVE PROPAGATION IN A RANDOM MEDIUM, by L. A. Chernov. McGraw-Hill, 1960.

ELEMENTS OF THE KINETIC THEORY OF GASES, by E. A. Guggenheim. Pergamon Press, 1960.

BIBLIOGRAPHY ON PLASMA PHYSICS AND MAGNETOHYDRODYNAMICS AND THEIR APPLICATIONS TO CONTROLLED THERMONUCLEAR REACTIONS, compiled by J. D. Ramer. Maryland University, Engineering and Physical Sciences Library, 1959.

ULTRASONICS, by B. Carlin. 2nd ed. McGraw-Hill, 1960.

CAREERS IN PHYSICS, by A. W. Smith. Rev. ed. Long's College Book Co., 1960.

MECHANICS, by K. R. Symon. 2nd ed. Addison-Wesley, 1960.

CRYOPHYSICS, by K. Mendelssohn. Interscience, 1960.

BIOPHYSICAL SCIENCE, edited by J. L. Oncley. Wiley, 1959.

PROPERTY MEASUREMENTS AT HIGH TEMPERATURES, by W. D. Kingery. Wiley, 1959.

EINFÜHRUNG IN DEN WÄRME UND STOFFAUSTAUSCH, by R. G. Eckert. 2. Aufl. Springer, 1959.

DIFFRACTION GRATINGS AS MEASURING SCALES, by J. Guild. Oxford University Press, 1960.

THERMAL ENGINEERING, by H. L. Solberg. Wiley, 1960.

CHEMISTRY AND CHEMICAL ENGINEERING

ADVANCED ORGANIC CHEMISTRY, by G. W. Wheland. 3rd ed. Wiley, 1960.

LIQUIDS AND LIQUID MIXTURES, by J. S. Rowlinson. Academic Press, 1959.

PHYSICOCHEMICAL MEASUREMENTS AT HIGH TEMPERATURE, by J. O'M. Bockris. Academic Press, 1959.

THE SURFACE CHEMISTRY OF METALS AND SEMICONDUCTORS, edited by H. C. Gatos. Wiley, 1960.

EXPLORING THE STRUCTURE OF MATTER, by J. J. Trillat. Interscience, 1959.

SYMPOSIUM ON THE MECHANISM OF HETEROGENEOUS CATALYSIS. Proceedings. Elsevier, 1960.

PULP AND PAPER, by J. P. Casey. 2nd ed. Interscience, 1960.

SUBSTITUTION AT ELEMENTS OTHER THAN CARBON, by C. K. Ingold. Weizmann Science Press of Israel, 1959.

CHEMISTRY OF SYNTHETIC DRUGS, by P. May. 5th ed. Longmans, 1959.

POLYTHENE, by A. Renfrew. 2nd ed. Interscience, 1960.

POLYSTYRENE, by W. C. Teach. Reinhold, 1960.

MOLECULAR STRUCTURE, by J. C. D. Brand. Arnold, 1960.

ELECTRICAL ENGINEERING

TRAVELING-WAVE ENGINEERING, by R. K. Moore. McGraw-Hill, 1960.

ELECTRONICS AND NUCLEONICS DICTIONARY, by N. M. Cooke. McGraw-Hill, 1960.

A SIMPLIFIED TECHNIQUE OF CONTROL SYSTEM ENGINEERING, by G. K. Tucker. Minneapolis-Honeywell Regulator Co., Brown Instruments Division, 1960.

PRINCIPLES OF FEEDBACK CONTROL, by C. H. Wilts. Addison-Wesley, 1960.

ANALYSIS AND DESIGN OF FEEDBACK CONTROL SYSTEMS, by G. J. Thaler. 2nd ed. McGraw-Hill, 1960.

DICTIONARY OF AUTOMATIC CONTROL, by R. J. Bibbero. Reinhold, 1960.

MATERIALS SCIENCE

CERMETS, by J. R. Tinklepaugh. Reinhold, 1960.

FLAT ROLLED PRODUCTS II, edited by E. W. Earhart. Interscience, 1960.

TIN AND ITS ALLOYS, by E. S. Hedges. Arnold, 1960.

REPORT ON STRESS-CORROSION CRACKING OF AUSTENITIC CHROMIUM-NICKEL STAINLESS STEELS. American Society for Testing Materials, 1960.

SYMPOSIUM ON PARTICLE SIZE MEASUREMENT. American Society for Testing Materials, 1959.

SYMPOSIUM ON ELECTRON METALLOGRAPHY. American Society for Testing Materials, 1960.

SYMPOSIUM ON EDUCATION IN MATERIALS. American Society for Testing Materials, 1960.

SYMPOSIUM ON EFFECT OF WATER-REDUCING ADMIXTURES AND SET-RETARDING ADMIXTURES ON PROPERTIES OF CONCRETE. American Society for Testing Materials, 1960.

SYMPOSIUM ON DURABILITY AND WEATHERING OF STRUCTURAL SANDWICH CONSTRUCTIONS. American Society for Testing Materials, 1960.

SYMPOSIUM ON NEWER METALS. American Society for Testing Materials, 1960.

SYMPOSIUM ON FATIGUE OF AIRCRAFT STRUCTURES. American Society for Testing Materials, 1960.

SYMPOSIUM ON TREATED WOOD FOR MARINE USE. American Society for Testing Materials, 1960.

DESIGN OF STEEL STRUCTURES, by B. Bresler. Wiley, 1960.

SYMPOSIUM ON THE THEORY OF THIN ELASTIC SHELLS. Proceedings. Interscience, 1960.

METALLIC CORROSION INHIBITORS, by I. N. Putilova. Pergamon Press, 1960.

FLIESSPRESSEN VON STAHL, by H. D. Feldmann. Springer, 1959.

Artificial Reverberation.—Improvements in artificial reverberation promise to facilitate conversion of an ordinary auditorium into the acoustic equivalent of a full-sounding concert hall. This acoustic conversion, which introduces no undesirable side effects, is now being actively investigated at Bell Telephone Laboratories. As with other artificial reverberation, it is accomplished entirely by electronic means.

Called "colorless" artificial reverberation, its principles were outlined at a recent meeting of the Audio Engineering Society. Dr. M. R. Schroeder and Mr. B. F. Logan of the Laboratories' technical staff are jointly perfecting the new electroacoustic technique.

Artificial reverberation has been used for many years by recording companies, broadcasters, and room acousticians. For example, a typical user might be a radio station wishing to broadcast a recording of an outdoor concert or open-air summer music festival. At the broadcast studio, an artificial reverberator would be employed to introduce reverberations, or echoes, in an attempt to imitate the fullness of an indoor performance.

The usual artificial reverberator available today has detrimental fluctuations in its amplitude-frequency-response characteristic which deviate appreciably from that of a real room. Thus an unpleasant quality may be added to the reverberant sound, an effect sometimes similar to talking through a long barrel. To obtain natural-sounding reverberation, users have had to resort to reverberation chambers or other analog devices for producing the desired echoes.

However, based on extensive studies of the problem, Schroeder and Logan of the Laboratories' Visual and Acoustic Research Department employed all-pass filters with exponentially decaying transients. The resulting artificial reverberation responds equally to all frequencies. Spectral balance, or color of the reverberated sound is not altered. Hence it is called "colorless."

A concert-hall effect can be approximated in the home through artificial reverberation. To achieve this with a radio or phonograph two or more loudspeakers are desirable.

Messrs. Schroeder and Logan have conducted many colorless artificial reverberation experiments at the Laboratories. To facilitate their research, they are investigating various schemes using the magnetic core storage and the logic units of a large-scale digital computer as the artificial reverberator. The reverberated sound produced as the computer's output is evaluated subjectively by listening.

A related subject also under study by Dr. Schroeder is quasi-stereophony. This method achieves the fullness (but not the localization) of true stereophonic sound with only one audio channel. Electroacoustic devices that produce this effect without discoloring the sound have been successfully built and demonstrated at the Laboratories.

A New Atomic Clock.—Three Harvard scientists have built a new kind of "maser" which promises to be over 100,000 times more accurate than the best atomic clock now running.

The heart of the new device is an ingenious "bouncing box" that stores high-energy-level hydrogen atoms long enough for them to emit a detectable wave of radiation of precisely 21-cm. wavelength.

The maser can be used both as a sensitive amplifier or as a source of 21-cm. radiation of unprecedented stability and purity of tone. The nearly perfect "monotone" it emits promises to be the most accurate timepiece in the world, a new standard for time or for frequency.

The accuracy of the new atomic maser has not yet been measured since with the best clock in the world, there is only one way to test its accuracy: build another identical clock and see how well they keep time with each other. A second atomic maser is now being built. It is hoped eventually that the accuracy will be one part in 10^{15}.

The new maser built by the Harvard scientists is the first to use free atoms, rather than atoms trapped in molecules or crystals. The radiation that the free hydrogen atoms give off is much purer than that emitted by other masers; interaction among atoms held in a molecule or a crystal tends to blur or spread out the frequencies they emit.

The hydrogen atom is made up of a proton and an electron. Because both are spinning, each acts as a tiny magnet. In a hydrogen atom, the magnetic axis of the proton can point either the same way as, or the opposite direction from, the magnetic axis of the electron. When the two magnetic axes flip from the parallel or high energy orientation to the anti-parallel position, the atom emits a photon of 21-cm. wavelength.

Here is how the atomic hydrogen maser works: A stream of hydrogen atoms is sent through a magnetic field that reflects those hydrogen atoms at the high energy state into a unique storage box. Since the radiation given off by the hydrogen is very weak, the trick is to keep the atoms in the high energy state for a long time—until enough have accumulated to give off a detectable chorus of 21-cm. radiation.

Ordinarily, the hydrogen atoms, bouncing off the sides of the box, would interact with the surface and quickly drop to the lower energy level. The new device has a special "bouncing box" a quartz bulb coated on the inside with a paraffin that does not very readily interact with the bouncing atoms. The scientists have found that one high-energy-level hydrogen atom can endure at least 10,000 bumps in this storage box, a life-time of about one second.

In this way, a large number of high-energy-level hydrogen atoms is stored up. The gas will then spontaneously emit a nearly perfect "monotone," thus acting as an oscillator or source of 21-cm. waves. But by deliberately decreasing the number of atoms present, this spontaneous emission may be checked. Then the device will emit 21-cm. radiation only when it is triggered by an incoming signal of the same wavelength, making the "bouncing box" a powerful amplifier.

An atomic clock, essentially an atom or a molecule that emits radiation, is the most accurate kind of timepiece known. Its "pendulum" is the very steady stream of pulses, or waves, it sends out.

As an oscillator, the new device will be used to measure some of the subtle physical properties of the protons, electrons and neutrons in atoms much more accurately than has been possible before. The Harvard men plan to study the interaction between the nucleus and its orbiting electron in deuterium and tritium (heavy isotopes of hydrogen).

In another experiment, they will deliberately force into the storage box an excess of hydrogen atoms to study and measure the interactions among them. These same interactions occur in the great clouds of hydrogen, in and between galaxies, that also broadcast on the 21-cm. wavelength.

The device could also be used to measure, to a much higher precision than has yet been possible, the effect of both gravity and speed on time, which was predicted by Einstein.

The atomic maser might eventually be of use in long-range communication. Such an amplifier in an earth satellite could be used to bounce signals from earth to another point. Because the amplifier's radiation is so pure, its range would be enormous.

The research was sponsored by the National Science Foundation and the Office of Naval Research.

Plasma Accelerator Tested.—A "plasma gun," built to test new ways of keeping future space vehicles travelling steady during flight, was fired continuously nearly four million times during a test at General Electric's Missile and Space Vehicle Department in Philadelphia.

Scientists at the department's Space Sciences Laboratory said the machine operated without stop for 18½ hr. and estimated it provided enough thrust during the test to stabilize a far-travelling spacecraft for two years. The thrust, or recoil, from the firings would be used to stop unwanted spinning and tumbling motions.

The equipment is called REPPAC which stands for Repetitively Pulsed Plasma Accelerator, and its test for more than 18 hours is believed by the laboratory to have set a record for this type of apparatus.

The new type of plasma propulsion will have a big advantage over the more conventional rockets and gas jets which have already been successfully used to stabilize space vehicles and satellites, according to General Electric scientists because:

The plasma accelerator shoots off a very energetic stream of material at extremely high speeds to obtain thrust, and a small amount of this material (plasma) goes a long way. Conventional gas jets or rockets obtain thrust by shooting off comparatively large amounts of material at much lower velocities, and thus much more fuel or compressed gas has to be stored. As the length of time of the space flight increases the jet and rocket methods become more undesirable because of weight and storage space limitations.

The plasma (a gas whose atoms have been broken up) reacts with a powerful magnetic field which accelerates the gas particles 50 times a second and discharges them at more than 22,000 miles per hour to produce thrust.

The REPPAC's "gun" is a T-shaped tube in which small amounts of gas are turned into the plasma and propelled into a vacuum chamber by a combination of electrical charges and a magnetic field.

All-Glass Insulating Paper.—New applications are demonstrating the ability of AMF's Tissuglas—an all-glass insulating paper—to solve unusual electrical, thermal, and electronic problems. Tissuglas, a product of American Machine & Foundry Company, is available in thicknesses as low as 0.0006 of an inch. It is uniform in texture and electrical resistance.

The newest, and potentially largest, application of Tissuglas is as a base for electroluminescent lamps. These lamps are flexible panels as thin as $\frac{1}{16}$ of an inch. The resulting lamps are

said to be the brightest, clearest and most uniformly textured light of any electroluminescent panels on the market today.

Another new application of Tissuglas is in the manufacture of bonded strain gages. Tissuglas, in this application, is used as a saturating base. In this use, its ability to pick up resins in uniform thicknesses (a function of its patented floc-free matting) gives the gages uniform resistance and high temperature stability.

Tissuglas is also finding a new market as a component for printed circuit materials. In this application, Tissuglas is laminated with a very thin copper foil. As an example, the one mil Tissuglas together with the ¾ mil copper produce the thinnest and most flexible printed circuit material now available.

Tissuglas is a sheet of matted submicron glass fibers made on a specially adapted paper making machine. It has very unusual properties as an insulating material: melting temperature above 1,200 degrees F.; thicknesses from ultrathin (.0006 in.) to .012 in.; pore sizes from 8 to 90 microns; and a dielectric of 370 to 2,370 volts. Produced in any width up to 38 in. and in continuous rolls.

Electronic Telephone Service.—A customer trial of the world's first electronic telephone central office (ECO) was started in mid-November of 1960 by Bell Telephone Laboratories and Illinois Bell Telephone, at Morris, Ill.

Developed by Bell Laboratories, it is the first system which performs electronically all the functions in handling of telephone calls. It was described by Bell Laboratories President James B. Fisk as " . . . a totally new system making possible a variety of new services which will double the flexibility and hence the potential value of each customer's telephone."

Through the use of tiny gas tubes, a vast memory system, and thousands of transistors and other solid state devices, which operate in millionths of a second, ECO permits Morris trial users to:

—Use home extension phones as intercoms, simply by dialing two digits.

—Reach frequently called numbers by dialing only two digits instead of seven.

—Have incoming calls routed to another phone when the original called line is busy.

—Dial a code which causes all subsequent incoming calls to be automatically transferred to any other number. (For example, to a friend's home if you went there for the evening.)

Other new services expected to be introduced after the trial is under way will permit many of the trial customers to:

—Allow a third party to be called into an existing telephone conversation.

—Have an immediate connection to a busy line as soon as the line becomes available.

Information gained from the Morris trial will tell not only how ECO performs, but it will also give an insight into which of the new service features telephone users prefer. Telephone engineers are now investigating ways to provide some of these new services through existing telephone systems.

The trial will also present an opportunity to study the kinds of maintenance activity and the number of people needed to operate and maintain the new exchanges. During the trial, the Morris ECO will be operated jointly by Illinois Bell and Bell Laboratories.

In appearance, ECO has little in common with present exchanges. The

long, high, racks of equipment and the noisy chatter of relays are gone. Instead, there are several rows of neat gray cabinets filled with thousands of plug-in packages of electronic components. The switching network, made up of 23,000 tiny, neon-filled tubes, goes about its work quietly, with only a bright red glow to show which tubes are operating.

One of the keys to the success of the ECO is that it uses *stored program control* to perform its job—that is, each action of the machine is determined by instructions stored in its memory.

The difference between ECO's stored program control and present systems can be simply illustrated by the two different ways a student can solve a square root problem. One way is by a series of logical steps—pointing off two places, etc. The other way is by looking up the answer in a book of square root tables.

Existing exchanges use the first method to work out the detailed logic of each telephone call, item by item. The ECO, on the other hand, solves many of its problems by "looking up the answer in the book." In this case the "book" is information—2¼ million bits—stored on photographic plates in the machine's memory, telling it what to do in any situation.

Because of ECO's extreme flexibility, it is capable of offering new and different services.

The ECO performs its work with such speed that it has enough "spare" time to continually check its own circuits. When it discovers a fault, it locates and diagnoses the trouble and, in some cases, even makes the necessary corrections. If the fault can't be corrected by the machine, it writes out in detail on a Teletypewriter what the trouble is, adding the month, day, hour, and minute of the malfunction. Then the repairs are made by a member of ECO staff.

Although some of its basic theory has been known for many years, ECO became feasible only with the invention of the transistor and other semiconductor devices, and with the development of high speed, high capacity memory systems. To illustrate the importance of semiconductors to the system it has only to be noted that the Morris ECO uses some 12,000 transistors and 105,000 diodes. It uses other electronic components by the tens of thousands.

Although the Morris ECO is an experimental version, Bell engineers are already at work on a production model, suitable for volume manufacture by the Western Electric Company. Many components in the production model will differ from those used at Morris, but the over-all philosophy of the two systems will be similar. The first production model will be operating by mid 1965, and from that time on ECO will gradually be introduced into the Bell System to meet the needs of telephone growth and to replace worn-out central offices.

Teaching Devices Demonstrate Physics Principles.—Two new laboratory demonstration pieces suggested by a prominent instructor to help teach physics students about changes created by thermal energy are now being made by Central Scientific Co., Chicago. One of the devices demonstrates the forces involved in thermal expansion and contraction while the other shows the effects of temperature change on the resistance of conductors.

Both were developed by Julius Sumner Miller, professor of physics at El Camino College, California, who brought them to Central Scientific. Cenco makes and markets many similar laboratory instruction pieces.

The thermal expansion and contraction unit is the No. 77430 Cenco-Miller Forces in Thermal Expansion Apparatus. This unit is built around a steel expansion bar about 1 ft. long, held between two ends of a yoke. The rod can be heated by a manifold gas burner built into the apparatus; it can be cooled either by the surrounding air or by spraying water on it.

In the test, cast iron drive pins are inserted in the rod at the free end, one on each side of the yoke end piece. As the heated rod expands, its pressure is exerted against the inside drive pin, causing it to break with an audible snap. On contraction, the other pin will snap.

Built of heavy duty material for years of use, this large demonstration (16½ in. long) can be seen throughout the classroom.

The other demonstration is the No. 83064 Cenco-Miller Temperature Coefficient of Resistance Apparatus. In this device, one of the two wires leading to a 6-volt 32-candlepower lamp consists of resistance wire wound around two rods so that the wire forms a bed. A tubular gas burner beneath this wire bed heats it, causing the resistance to increase and the light to go out. Cooling causes the lamp to brighten. This unit is 16½ in. long.

In addition to these demonstrations of thermal effects, two other Cenco-Miller devices demonstrating rotational forces are now available from Cenco. For additional information about any of the new Cenco-Miller demonstration devices, write to Central Scientific Company, 1700 Irving Park Road, Chicago 13, Illinois.

Scrambling Device Blocks Bank Passbook Forgery.—A scrambling device which makes it virtually impossible to forge passbook signatures in the withdrawal of savings bank deposits and, at the same time, substantially reduces customer waiting time at tellers' windows has been announced by the Radio Corporation of America.

Known as Signaguard, the device reproduces a passbook signature as an unrecognizable mass of broken lines. When the passbook is presented at the teller's window, the device returns the signature to its original appearance for comparison with the customer's signature on the withdrawal slip.

Dr. H. J. Wall, Manager of RCA Applied Research at Camden, N. J., which developed Signaguard, said banks are expected to use the device in conjunction with electronic data-processing systems situated in their main offices.

This would eliminate the need for duplicate records of signature and account status in each branch office, he pointed out, and also would do away with time-consuming withdrawal checking procedures.

The new protection system, Dr. Wall said, makes use of fiber optics—glass tubes that carry light and images around bends and corners.

It so effectively scrambles a signature that even a bonafide depositor, much less an aspiring forger, cannot decipher the name on a lost passbook, he said. The imprint is produced as mixed segments of lines thousandths of an inch in diameter, corresponding to the diameter of the tubes.

As a double check, a secret number can be attached to the name. This effectively foils forgery attempts by persons who know the depositor well and can duplicate his signature.

The new device, Dr. Wall said, will make savings bank accounting foolproof. Another of its advantages is the elimination of tub files—files con-

taining cards on all depositors—which each teller must consult before completing a withdrawal. This, he said, would make for more room and less confusion in the banks, and would eliminate the time required to refer to such files for signature comparison and account checking.

Signaguard may be likened to a cable or telephone wires, with each individual wire being a glass tube instead of copper wire, the RCA official explained. Each tube picks up a small segment of the signature and transmits it to the other end of the tube via a devious route. This scatters signature segments throughout the unintelligible mass that is imprinted on sensitized paper at the other end of the tube.

In the bank the fiber optics tube is reversed to bring the scrambled signature back to its original form for comparison with the signature submitted to the teller.

Use of Signaguard in conjunction with the bank's central computer system, Mr. Wall said, would permit a teller to complete a banking transaction without leaving his window.

Applications, other than in savings banks, are contemplated for Signaguard, Dr. Wall said. It may be employed in identification cards for commercial bank depositors, for retail credit cards, and in-plant security.

Thermocouples for Low Temperature Applications.—A new line of gold-cobalt vs. copper thermocouples and complementary indicating, recording and controlling instruments for low temperature applications has been announced by Cryogenics, Inc., Washington, D. C.

Open and closed well thermocouples are available in ranges from 0–300°K, with accuracy of ±1 per cent of span or 2°K, whichever is greater. All are interchangeable to ±4°K. In special cases, the company notes, a spool of one continuous length prepared from the same melt is provided and held for customers, with all thermocouples being fabricated from this spool. In such situations, interchangeability of better than 2°K is guaranteed.

Direct Reading Instruments with internal reference junction compensation for use with these thermocouples are also available, in a choice of indicating, recording or controlling functions.

For additional information, write Cyrogenics, Inc., 1129 Vermont Ave., N. W., Washington 5, D. C.

Commercial Gold Recovery Unit.—The first commercial unit for recovering gold lost in electroplating has been introduced by Technic, Inc., of Providence, R. I., one of the largest producers of precious metal solutions for plating.

Until now between 4 and 10 per cent of all gold used in electroplating has simply gone down the drain, and the loss to the plating industry runs to millions of dollars a year.

With the new unit, one electroplater, using the new special resin Gold Saver on a trial basis, will have recovered enough gold in less than three months to pay for the unit.

The Gold Saver, designed to become part of the gold-plating process, consists basically of:

—A column of special resin, small "BB" size particles, which capture gold in solution that now is being lost;

—A pump for circulating through the resin column the water in which the gold is dissolved; and

—Pipes, hoses, and connections between the pump and the special resin column.

After an item is plated with gold, it is immediately immersed in a tank

of water to rinse off and save the plating solution, which frequently costs between $40 and $50 a gallon. This "rinse" tank is called a drag-out tank.

Over a period of time, the concentration of gold solution in the drag-out tank builds up until, because of its gold content, it is worth possibly $10 a gallon. Periodically contents of this tank are added to the gold plating tank to keep the plating solution at a workable level and to recover some of the gold.

In the past, the plated item was then rinsed in running water, and the gold "drag-out" from the drag-out tank was lost.

The Gold Saver comes before this running water rinse.

The unit is attached to a tank into which the plated item is dipped, after the drag-out tank. The pump continuously circulates the solution through the special resin trap, where the gold is picked up.

The work, free of gold, is then rinsed in running water.

When the resin is completely saturated with gold it may be burned by the plater to recover the gold, sent to a refiner, who would also recover the gold by burning, or it may be returned to the Technic laboratories for reclaiming.

The Gold Saver is designed for any acid or non-free cyanide golds, such as Technic's 24K acid, Orotherm HT, Orosene 999, or HG non-free cyanide gold baths. Similar ion-exchange traps for cyanide golds, rhodium, palladium, and platinum already are under development or test.

New Cancer Treatment.—A new method for using cytotoxic drugs in the treatment of cancer has been developed by surgeons at the Royal Infirmary, Glasgow, Scotland. It has been applied successfully in four operations.

The use of cytotoxic drugs, developed in the U. S. as a cancer palliative by reducing the size of tumors, or in conjunction with surgery, has been limited up to now because it can be lethal; a dose strong enough to kill a tumor can sometimes also kill the patient.

The Glasgow surgeons have developed a technique to eliminate this danger by isolating the circulation in the affected part of the body. By so doing, 20 to 30 times the amount of cytotoxin can be administered than previously.

The surgeons are achieving palliation for two to four years of cancers which were previously incurable, and they are also able for the first time to investigate the properties of the cytotoxic substance. A hospital official said, "The work is not being duplicated elsewhere."

The method is still in the development stage.

YOU CAN ADVANCE SCIENCE EDUCATION

Today, more than ever before in its 135-year history, there is vital need for The Franklin Institute to effectively promote education in science and technology. It is imperative that we meet this challenge by providing adequate educational opportunities in these fields. This requires vision, objective planning, and money. We have more than enough of the first two requisites, but far too little of the third.

Our programs are aimed at professional scientists and industry, as well as the lay public and young people seeking inspiration and guidance in choosing a career. The Institute's educational programs are impressive, for they begin with students in the early grades of our elementary schools and continue throughout an individual's professional or industrial life. With more funds at our disposal, the scope and vigor of these activities could be greatly increased.

The Franklin Institute is not richly endowed. It is a non-profit organization, depending for encouragement and support on an understanding public. Capable and conservative management assures wise administration of all funds.

Your gift or bequest, large or small, will be deeply appreciated and will be used effectively to broaden the Institute's educational usefulness. There is a warm satisfaction in giving financial support to an organization that has pioneered in, and is dedicated to, the advancement of science and technology through education.

When property is transferred, title should be in the name of The Franklin Institute of the State of Pennsylvania for the Promotion of the Mechanic Arts.

The Secretary of The Franklin Institute will gladly furnish you with additional information. Write to him at The Franklin Institute, Benjamin Franklin Parkway at Twentieth Street, Philadelphia 3, Pennsylvania.